The *Chandra* X-ray Observatory

An Introduction

Nicholas Lee
Center for Astrophysics | Harvard & Smithsonian
Chandra X-ray Center—Science Data System

Chandra/CIAO Workshop—University of Massachusetts Lowell, May 19-23, 2025

CENTER FOR ASTROPHYSICS
HARVARD & SMITHSONIAN

Chandra

at a Glance…

CHANDRA
X-RAY OBSERVATORY

- best angular resolution of any X-ray satellite
  - sub-arcsecond (compare HST ~0.1 arcsec, *XMM-Newton* ~10 arcsec, ROSAT 5 arcsec)
  - good energy range and resolution (300 eV–9 keV) $E/\Delta E \sim 5 - 40$
- highest energy resolution (via gratings) of any X
  satellite up until *Hitomi*/XRISM were launched
  - $R = E/\Delta E$ ~1400–200, XMM RGS $E/\Delta E \sim$500–40
  - Radio and optical not uncommon to get $R \sim 20000$
- very high dynamic flux range:
  - sensitive to two orders of magnitude energy range,
  - 11 orders of magnitude flux sensitivity: 10^{-18}–10^{-7} ergs/cm^2/s

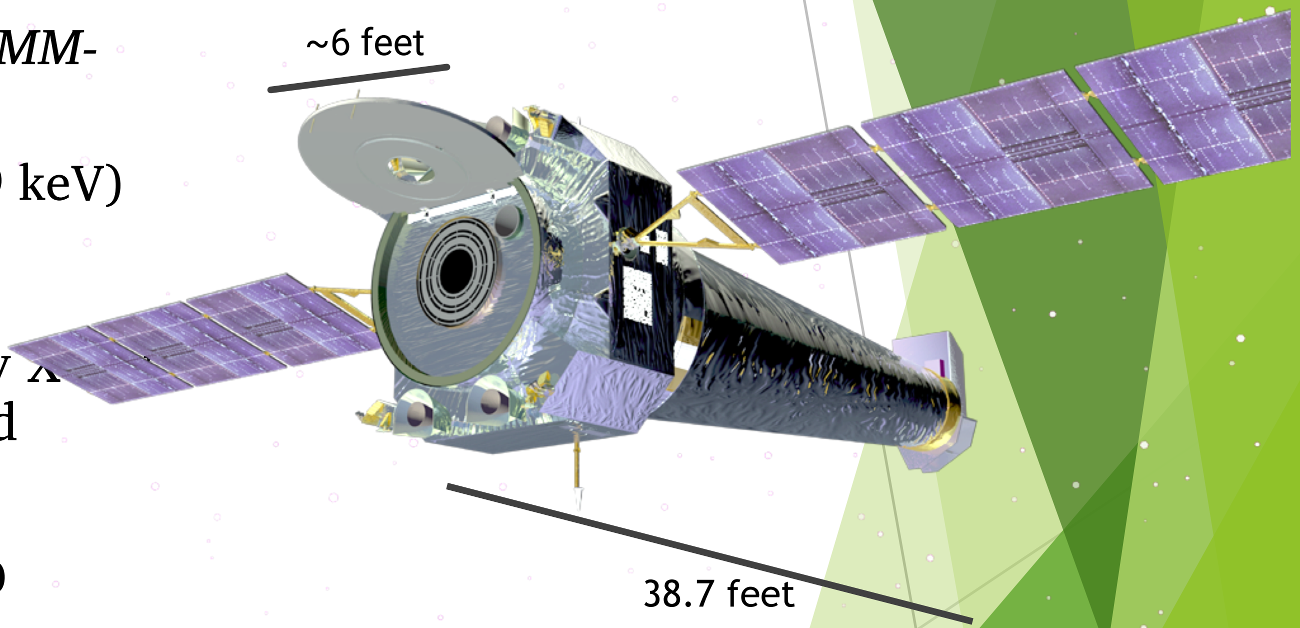

CHANDRA
X-RAY OBSERVATORY

Preliminaries

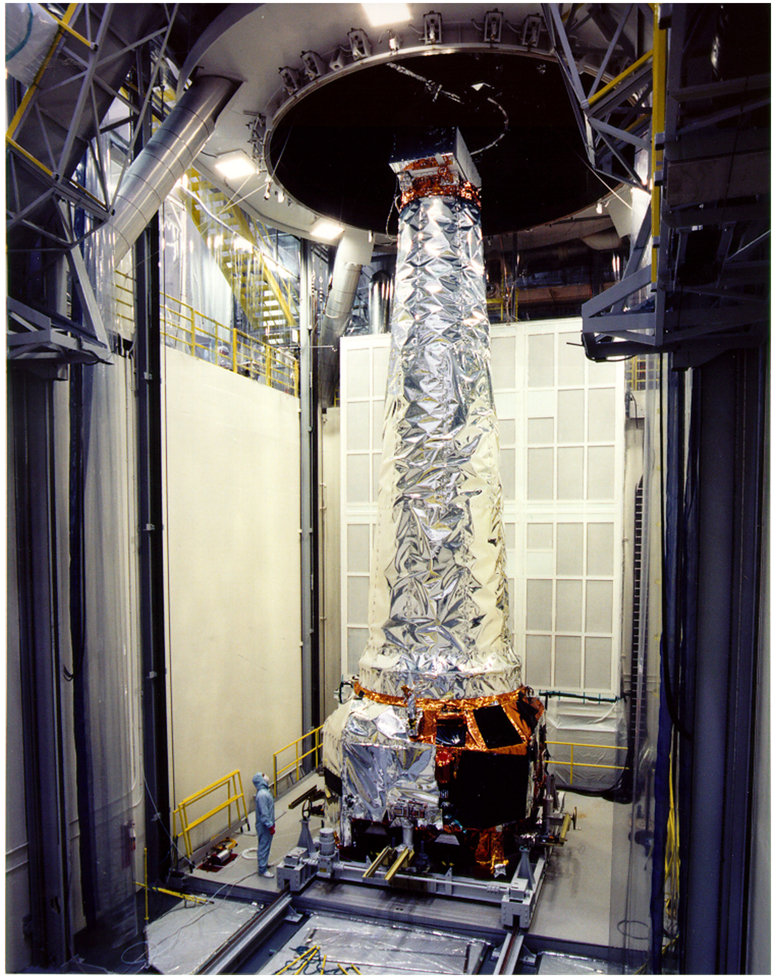

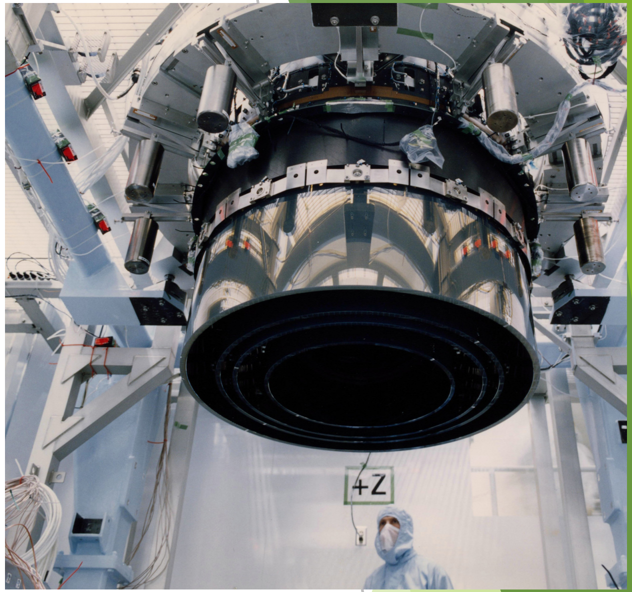

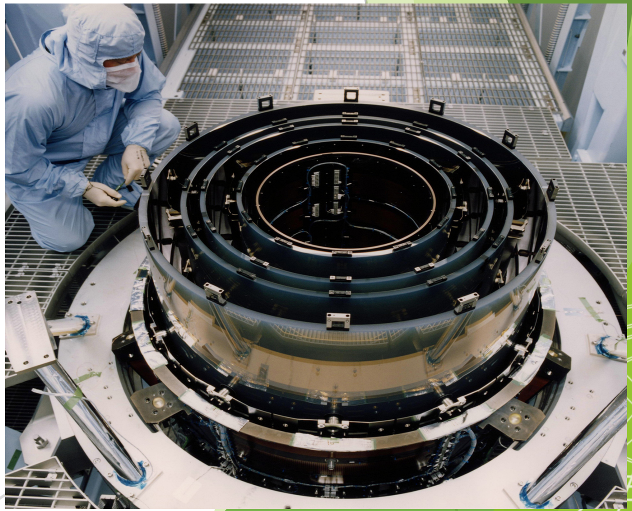

CENTER FOR ASTROPHYSICS
HARVARD & SMITHSONIAN

What are X-rays?

- "Soft" X-rays: 0.1-10 keV [$\lambda \sim 124$-1.24 Å]
  - reminder the Bohr radius is $a_0 = 0.529$ Å; X-rays are at *atomic scales*
- X-ray detectors are *photon counting*
  - the "events" table is the fundamental data product in high-energy astrophysics

Approximate Wavelength Ranges

γ-ray: ≤ 0.1 Å
X-ray: 100 Å ≥ 0.1 Å
ultraviolet: 100 Å – 3000 Å
optical: 1 μm – 3000 Å
infrared: 100 μm – 1 μm
mm/sub-mm: 10 mm – 0.1 mm
radio: 100 m – 1 cm

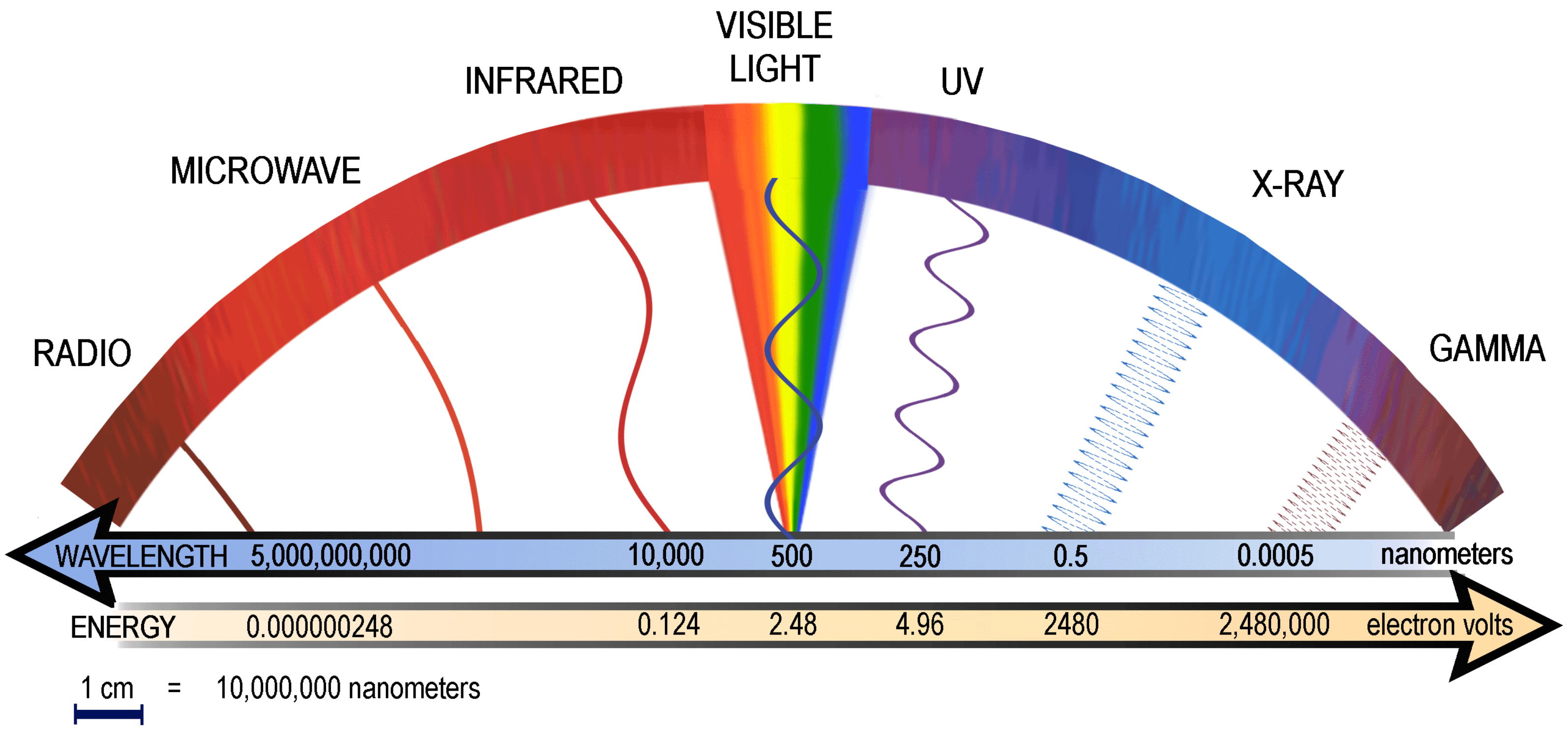

Photon counting is possible since X-rays are relatively easy to detect given the large energies and they have relatively low fluxes, making it easier to count.

CHANDRA X-RAY OBSERVATORY

CENTER FOR ASTROPHYSICS HARVARD & SMITHSONIAN

Atmospheric Absorption

Cosmic X-rays Completely Attenuated by Photo-Electric Absorption of Air Molecules

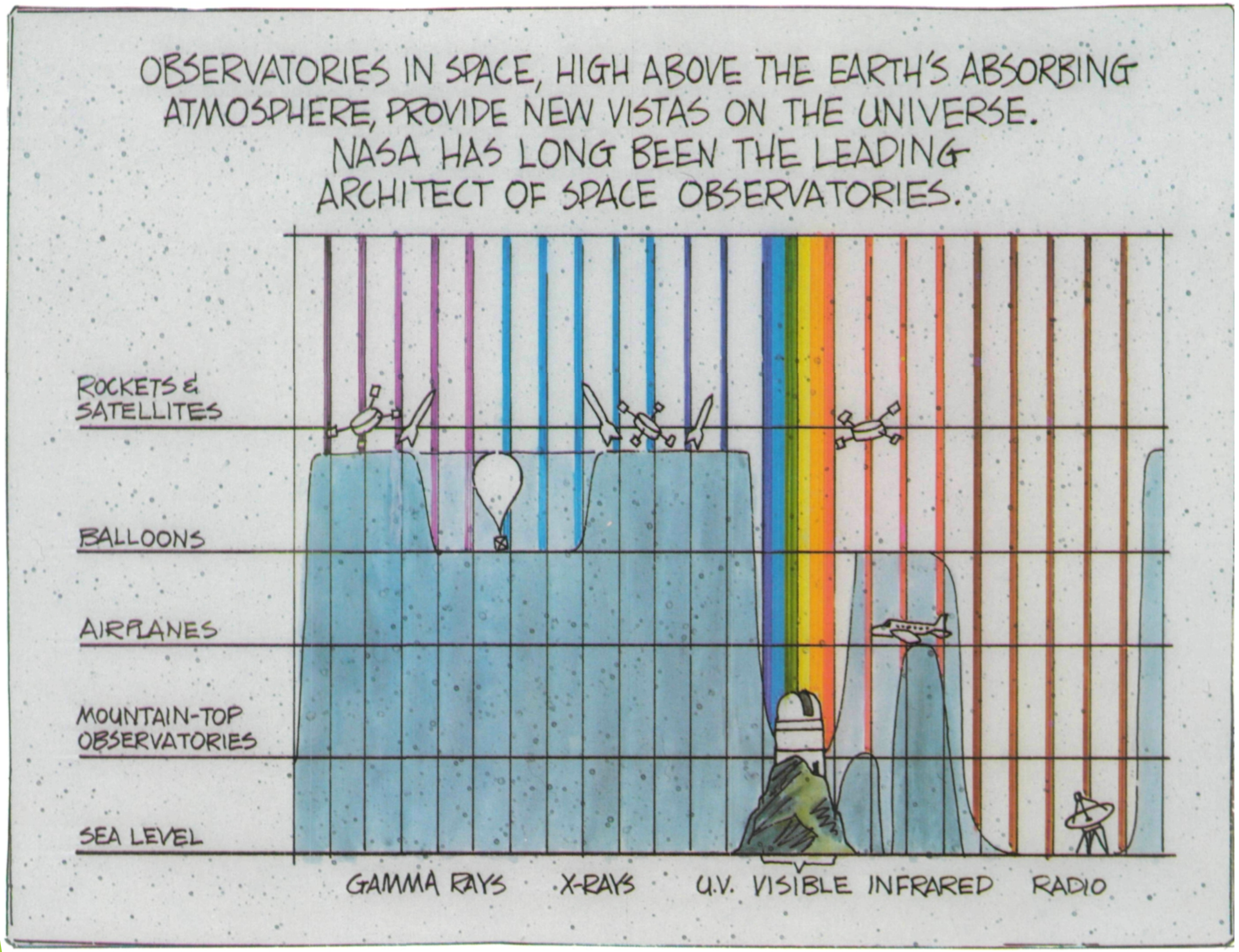

Beer-Lambert law:

$$I = I_0 e^{-\mu d}$$

for linear attenuation of radiation beam.

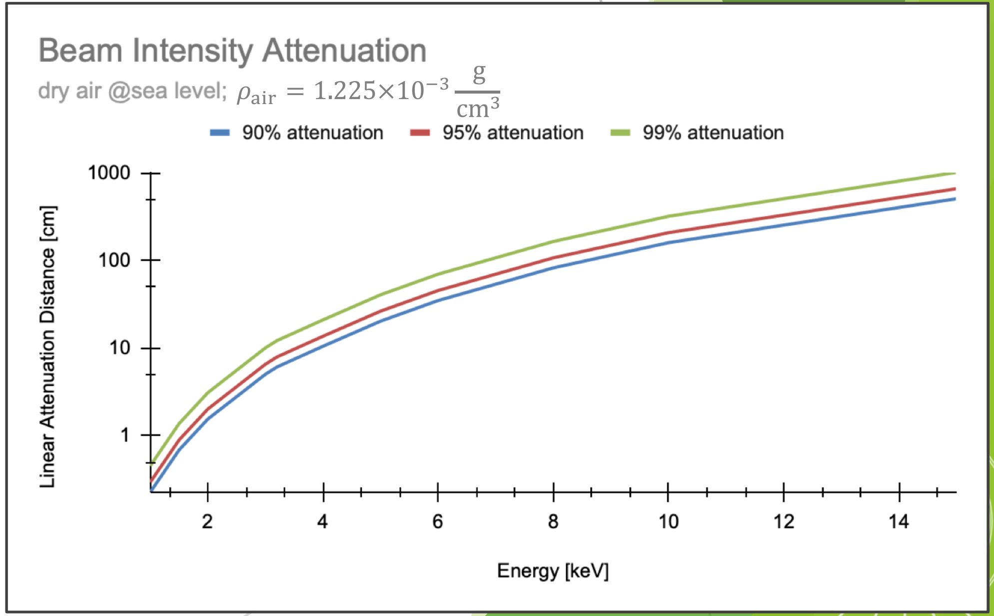

Why X-rays?

- what is being missed?
- multi-wavelength studies to rule out or validate models.
  - Non-detections has worth!
- TDAMM: time domain and multi-messenger astronomy.
  - i.e. identify gravitational wave mergers or type of GRB based on afterglow measurements
  - source localization
- astrophysics laboratory & laboratory astrophysics

AXAF the top priority from the 1980s Astronomy & Astrophysics Decadal Survey

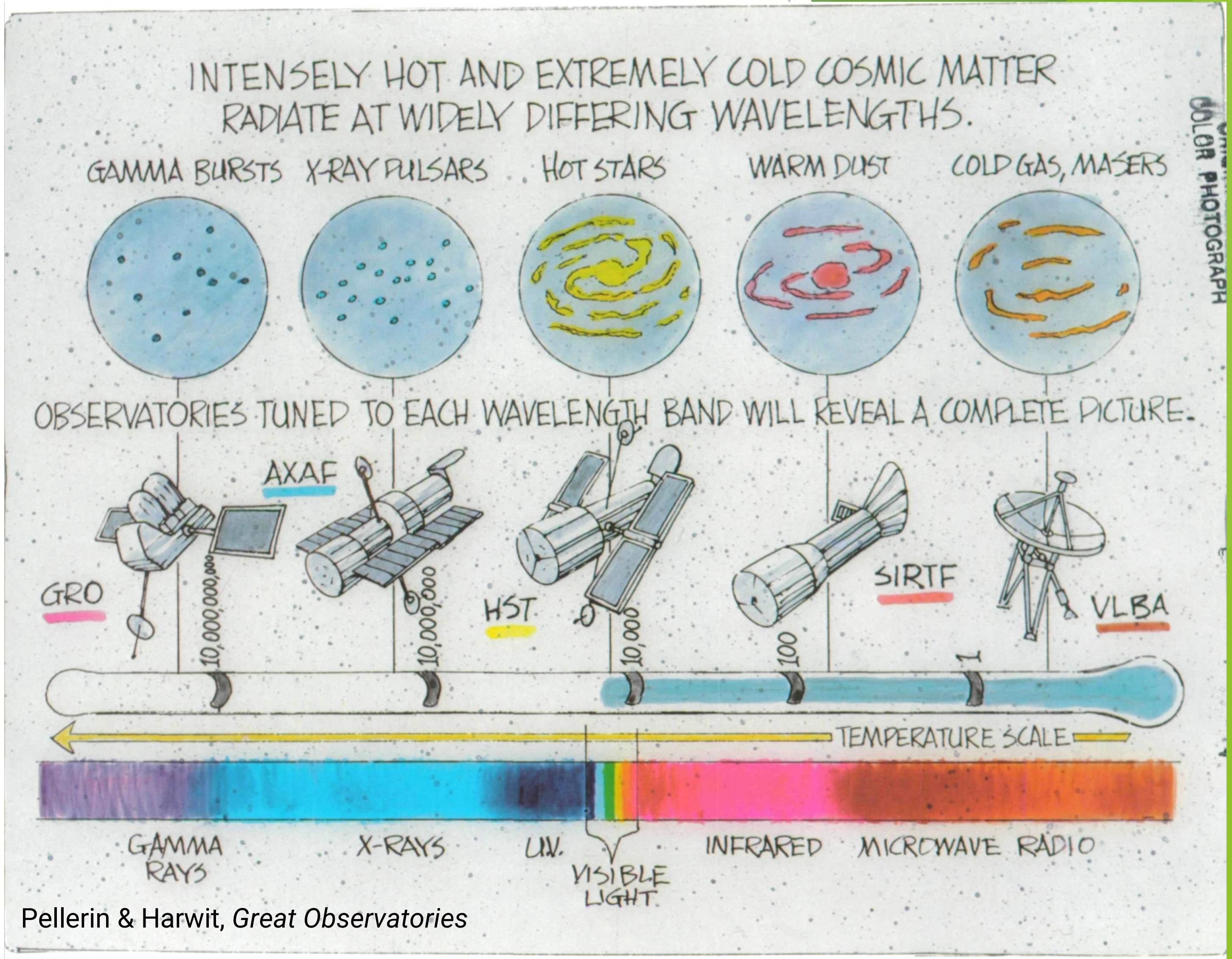

Pellerin & Harwit, *Great Observatories*

1980s Astronomy & Astrophysics Decadal Survey

CHANDRA
X-RAY OBSERVATORY

Program	1982 Status	Specifications	Problems Addressed
Solar Optical Telescope (SOT)	Selected by NASA as first major astrophysics facility for Space-lab; projected launch 1987-88	Ultraviolet, optical, near-infrared 10 x to 50 x ground-based angular resolution (0".1 at 5000 A, 0".02 at 1100 Å)	Dynamics of the solar photosphere, chromosphere and corona; solar magnetic field
Shuttle Infrared Telescope Facility (SIRTF)	Proposed NASA Spacelab facility recommended by CSAA	Infrared, submillimeter, 2-300-μm wavelength Wide field 103x sensitivity of present telescopes	Statistical study of infrared sources; molecular clouds and star formation; evolution of distant galaxies; planetary atmospheres
25-Meter Millimeter Wave Radio Telescope	Recommended by Greenstein report; next major ground-based facility projected by NSF long-range plan for astronomy chemistry	1-10-mm wavelengths Aperture, 25 m Located at high dry site	Interstellar molecular clouds and star formation; mass loss from stars; intergalactic gas in clusters of galaxies; interstellar
Major New Programs Recommended by Astronomy Survey Committee			
Advanced X-Ray Astrophysics Facility (AXAF)	Proposed Shuttle-launched, free-flying observatory	X-ray 100 x sensitivity and 10 x angular resolution of Einstein (HEAO-2) Capability for polarimetry High spectroscopic sensitivity and resolution	Stellar x-ray sources throughout Galaxy; x-ray sources in nearby galaxies; distant active galaxies nd quasars; clusters of galaxies; nature of x-ray background radiation; supernova remnants
Very-Long-Baseline (VLB) Array	Proposed ground-based facility	Radio wavelengths 100x angular resolution of any image-forming telescope	Compact objects in molecular clouds; center of the Galaxy; nuclei of galaxies; quasars; testing General Theory of Relativity; precise distance scale in Galaxy; geodesy and space navigation

regions. An urgent scientific need therefore exists for a long-lived satellite observatory with capabilities for x-ray astronomy that complement those of Space Telescope (ST) in the optical/ultraviolet region and those of the Very Large Array in the radio region of the spectrum.

The AXAF will fulfill that need with an instrument that utilizes the same basic principles that were tested and proved in the *Einstein* mission but which is capable of providing up to a hundredfold greater sensitivity for the study of faint stellar or quasistellar objects and a tenfold increase in angular resolution for the study of structure in extended objects. Major improvements will be achieved in spectroscopic sensitivity and resolution, and a capability for sensitive polarimetry will also be provided. The Space Shuttle will provide the means for launching AXAF, maintaining it in orbit, and retrieving it for major refurbishments. Thus, like ST, AXAF will be a national facility that can meet fundamental needs of astronomy for a decade or more.

AXAF will permit the observation of sources with x-ray luminosities as small as 1 percent of the Sun's total luminosity lying in the farthest reaches of our Galaxy, as well as the study of all the individual high-luminosity x-ray sources in the hundreds of galaxies of the Virgo cluster. The composition and dynamics of extended sources such as supernova remnants, galaxy halos, and clusters of galaxies can be revealed by spectroscopic and polarimetric observations of high angular resolution. The great sensitivity of AXAF will permit investigation of x-ray galaxies and clusters of galaxies out to distances so large that the effects of evolution in the early Universe should be apparent. Because of its power and versatility, AXAF will profoundly influence and enhance the development of nearly all areas of Galactic and extragalactic astronomy.

The Committee also suggests that NASA consider the establishment of special institutional arrangements similar to those embodied in the Space Telescope Science Institute, to provide scientific guidance for the development and maintenance of AXAF, to manage the scientific direction of the mission during orbital operations, and to facilitate the participation of the scientific community in the acquisition and interpretation of x-ray observations. Consideration should be given, as in the case of the Space Telescope Science Institute, to appropriate international participation.

2. A Very-Long-Baseline (VLB) Array of Radio Telescopes

The Astronomy Survey Committee recommends the construction of a ground-based Very-Long-Baseline (VLB) Array of radio telescopes

CENTER FOR ASTROPHYSICS
HARVARD & SMITHSONIAN

Multi-Wavelength View of the Crab Nebula

CHANDRA X-RAY OBSERVATORY

CENTER FOR ASTROPHYSICS HARVARD & SMITHSONIAN

Multi-Wavelength View of the Crab Nebula

CHANDRA X-RAY OBSERVATORY

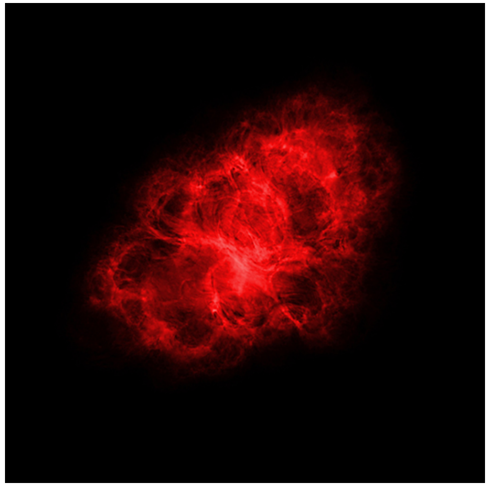

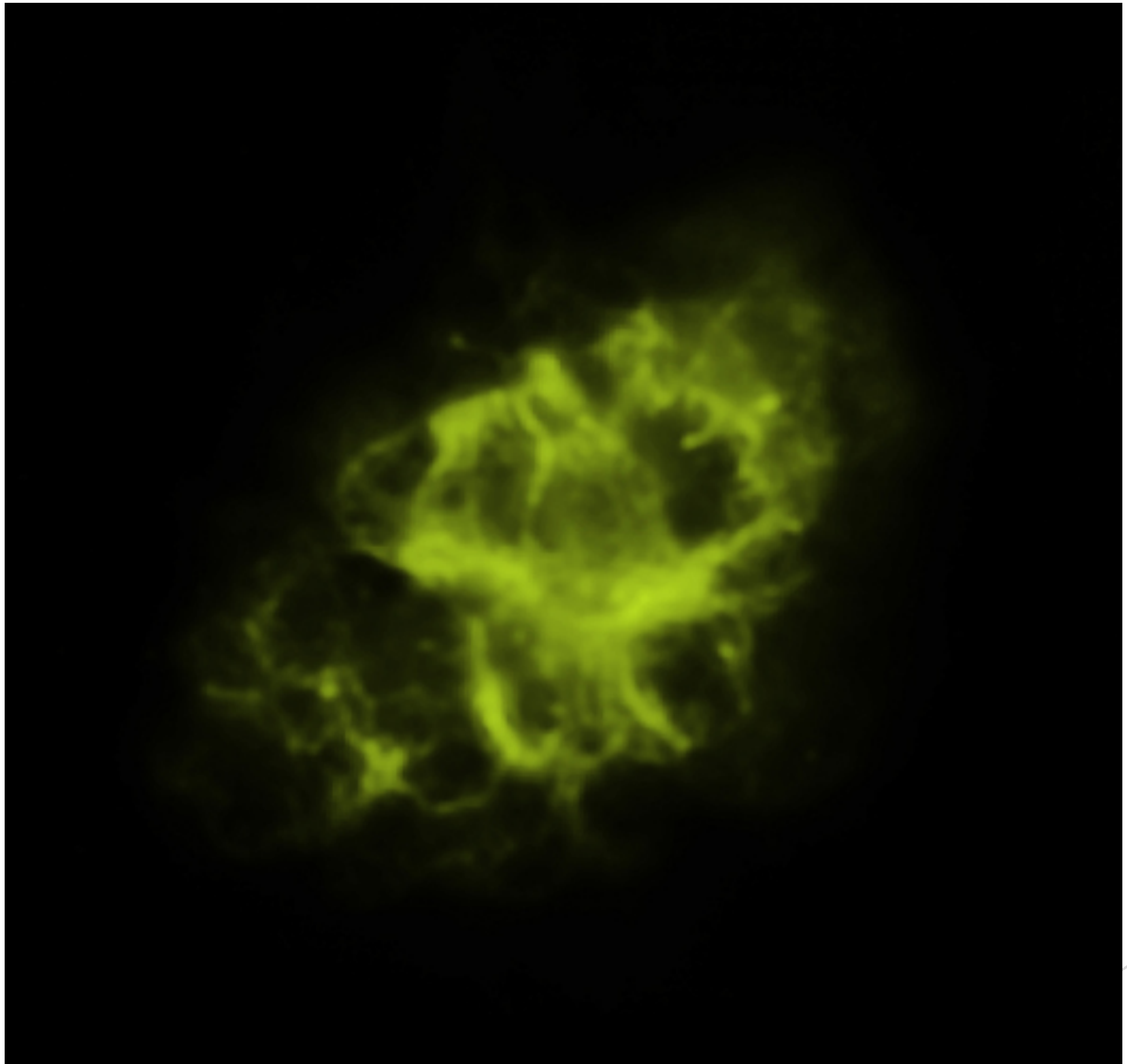

Spitzer (IRAC & MIPS 3.6, 4.5, 5.8, 8.0, 24, 70 μm)

CENTER FOR ASTROPHYSICS HARVARD & SMITHSONIAN

Multi-Wavelength View of the Crab Nebula

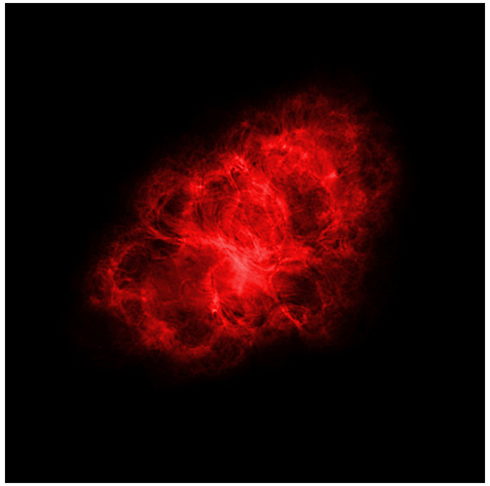

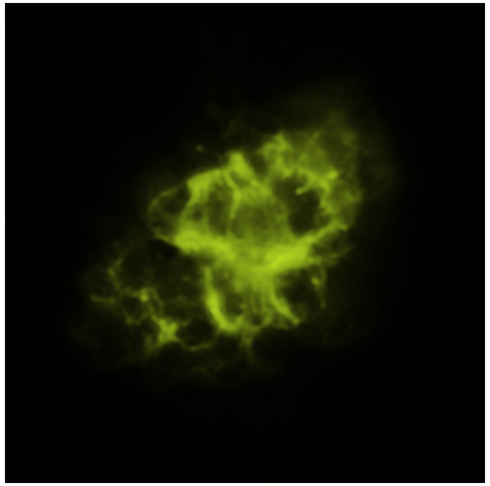

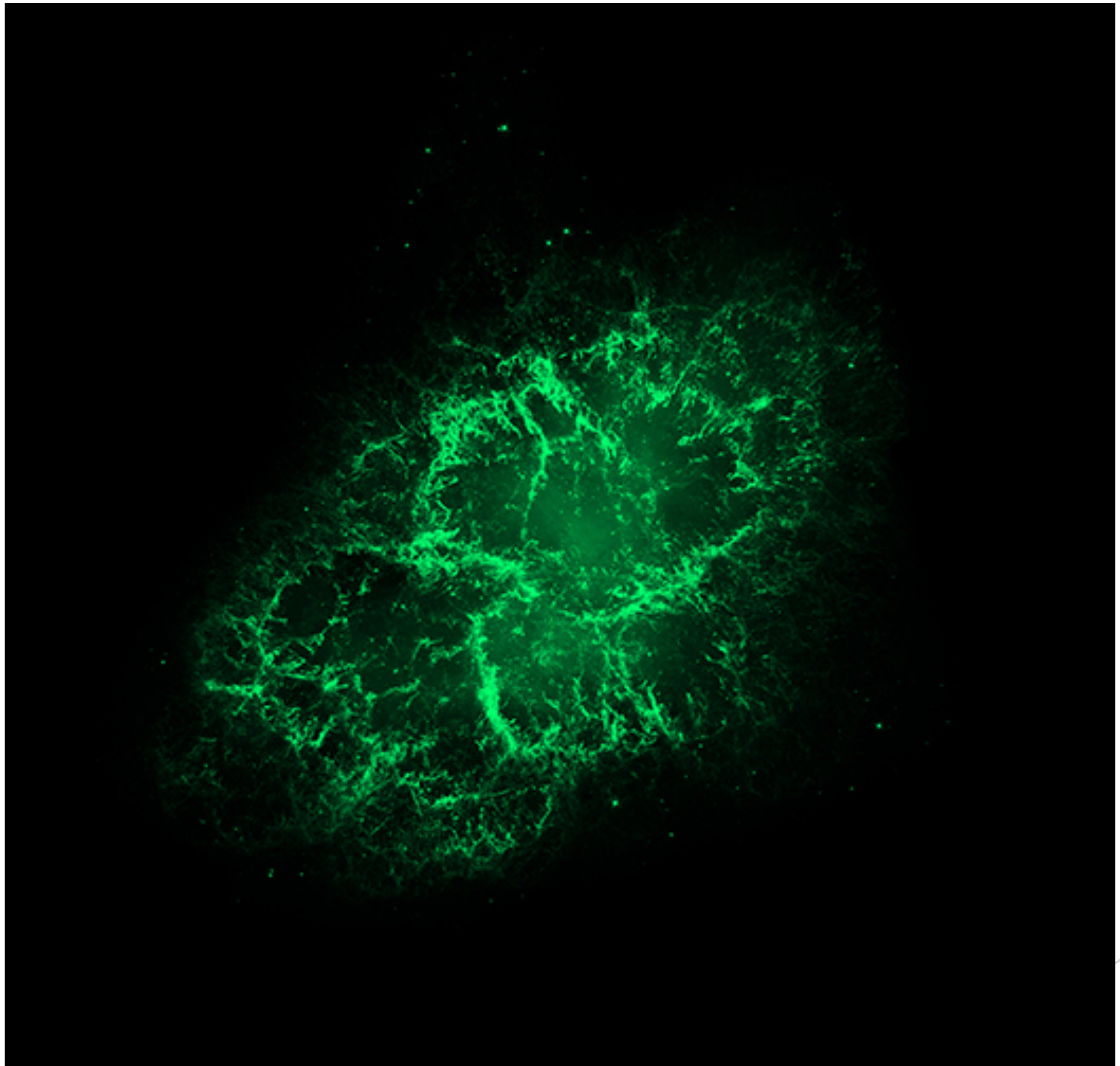

HST (WFPC2 F502N [O III], F673N [S II] F631N [O I], F547M continuum)

Multi-Wavelength View of the Crab Nebula

CHANDRA X-RAY OBSERVATORY

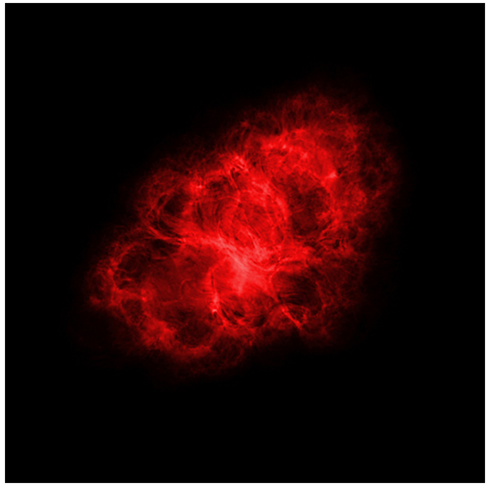

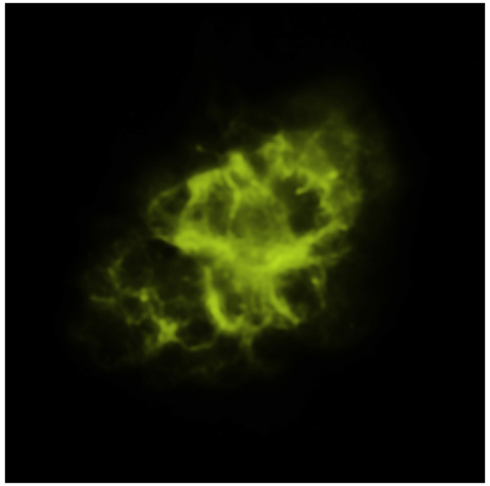

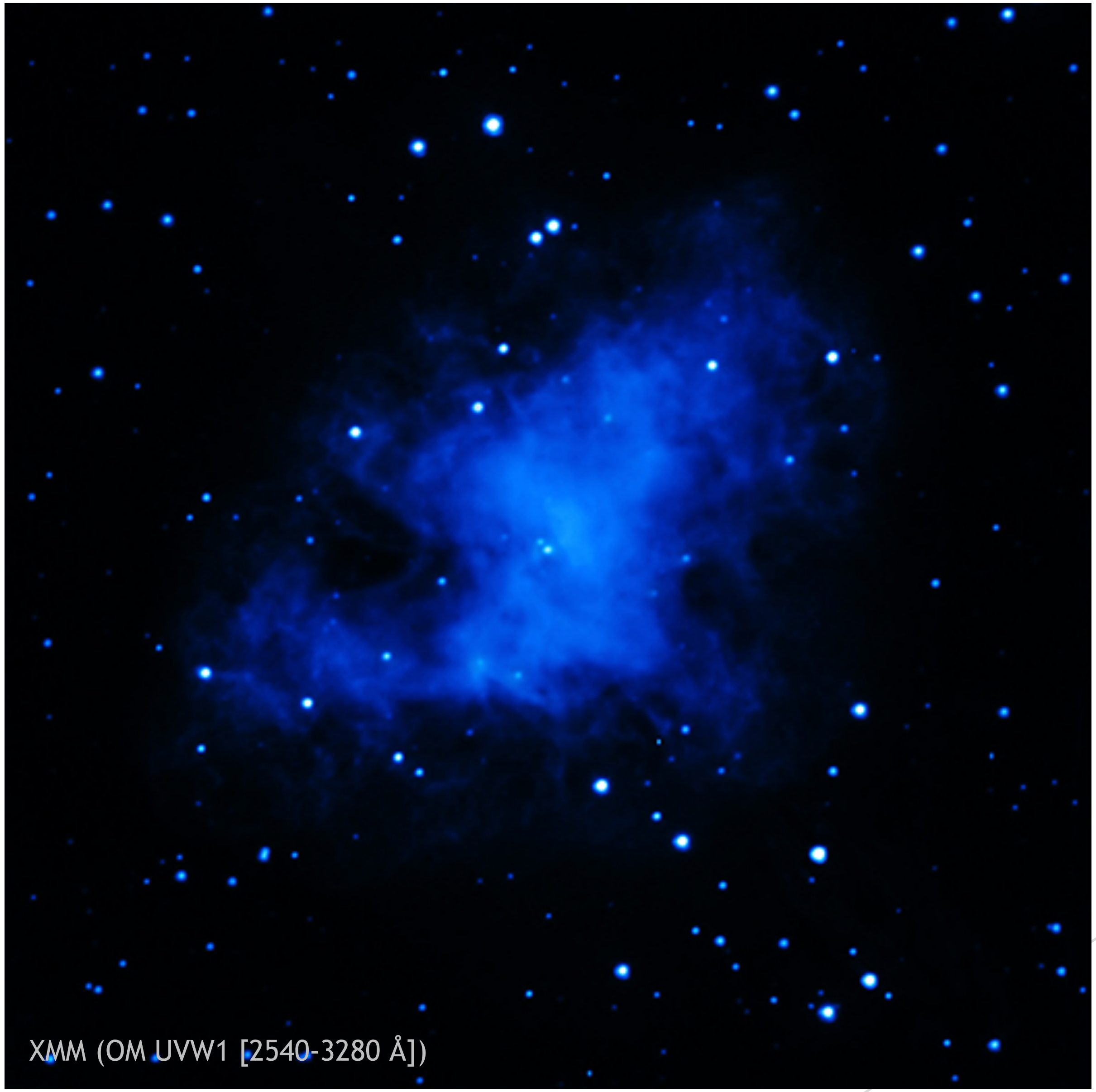

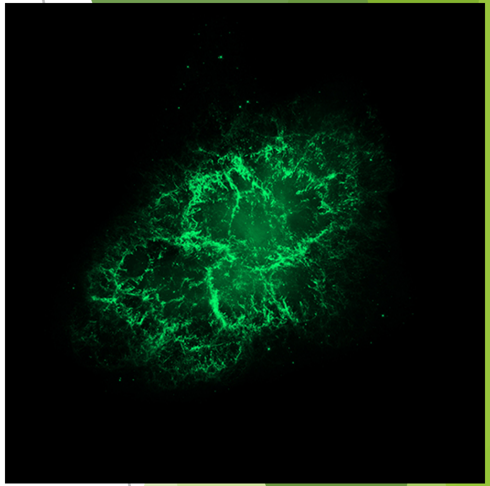

CENTER FOR ASTROPHYSICS HARVARD & SMITHSONIAN

Multi-Wavelength View of the Crab Nebula

CHANDRA X-RAY OBSERVATORY

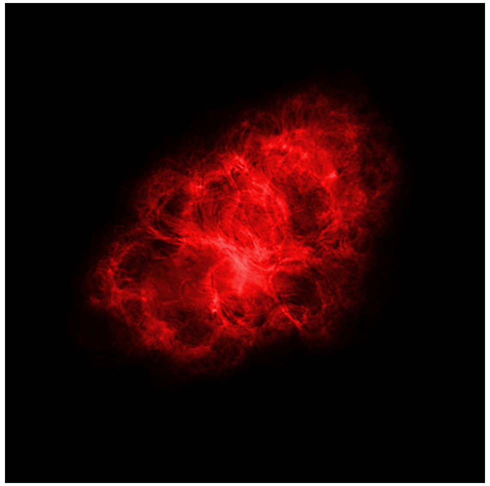

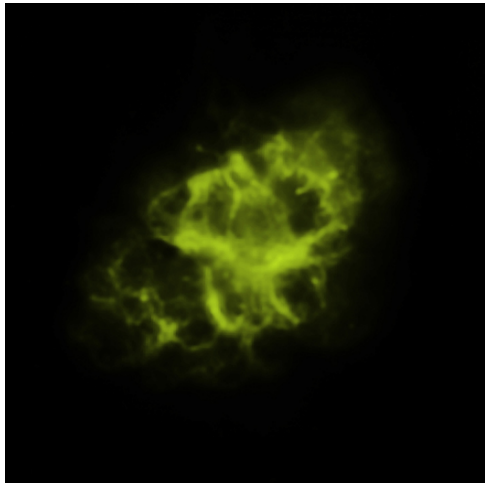

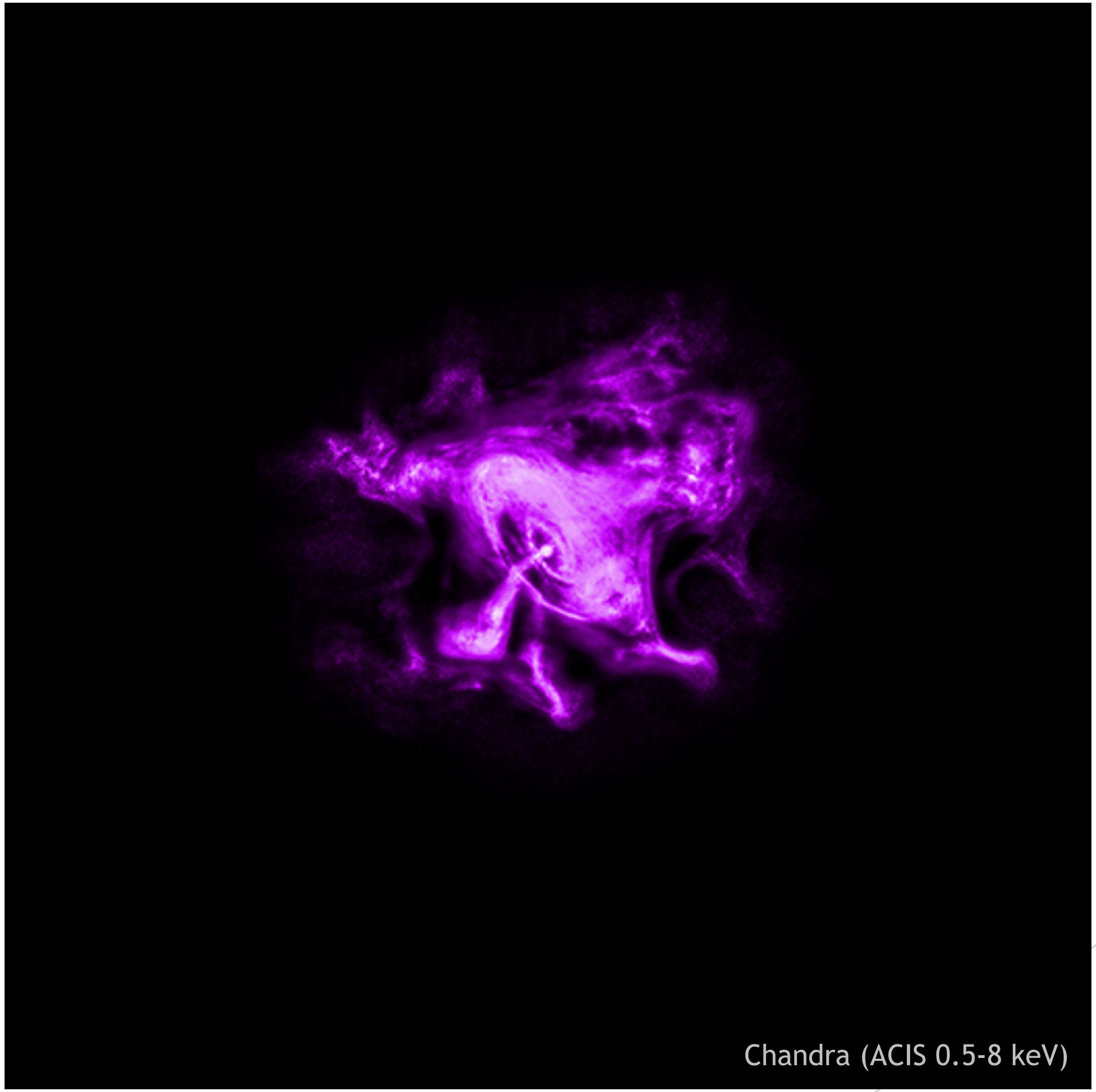

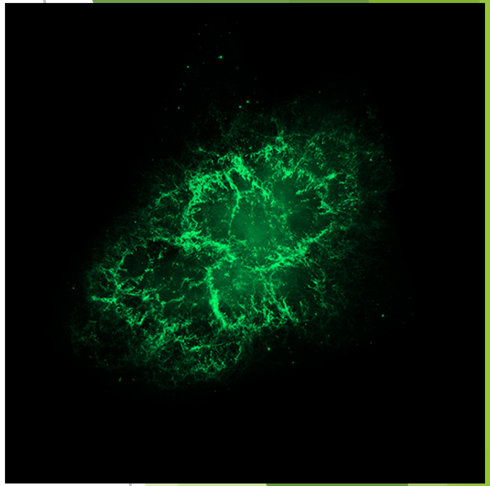

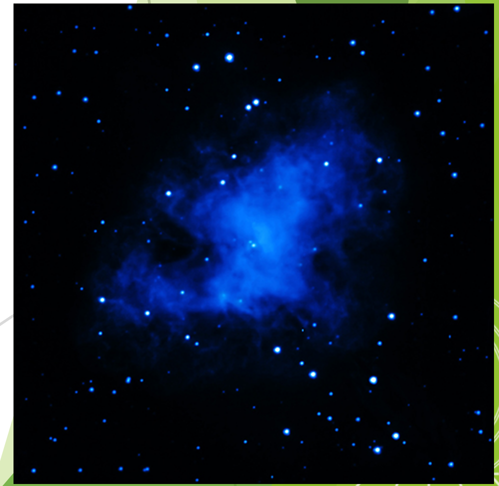

CENTER FOR ASTROPHYSICS HARVARD & SMITHSONIAN

How are X-rays Produced?

references…

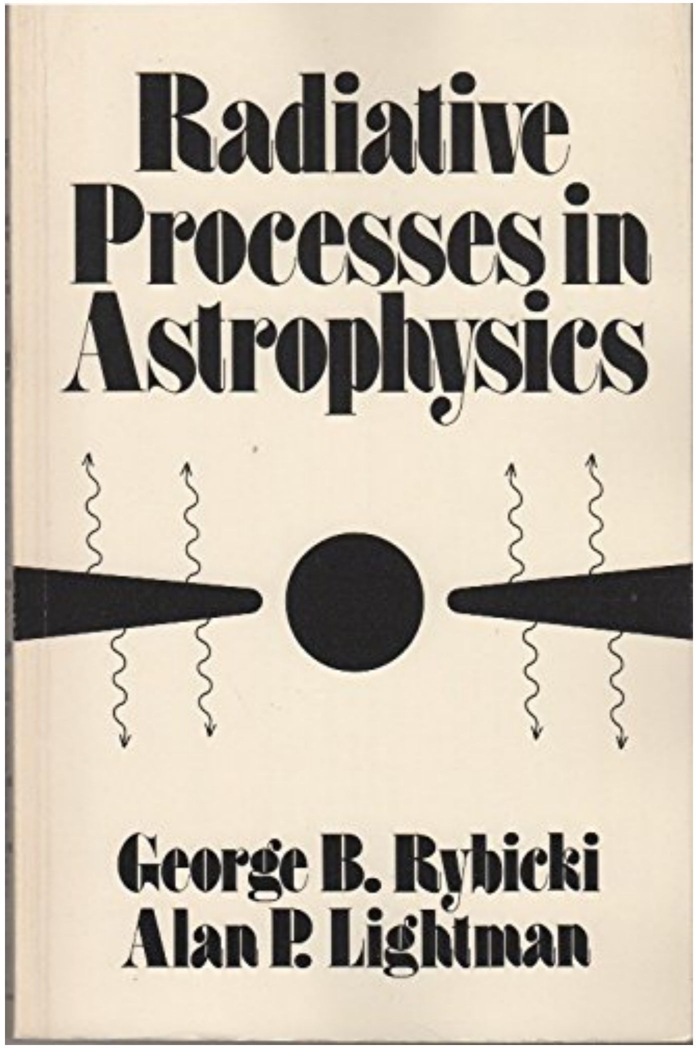

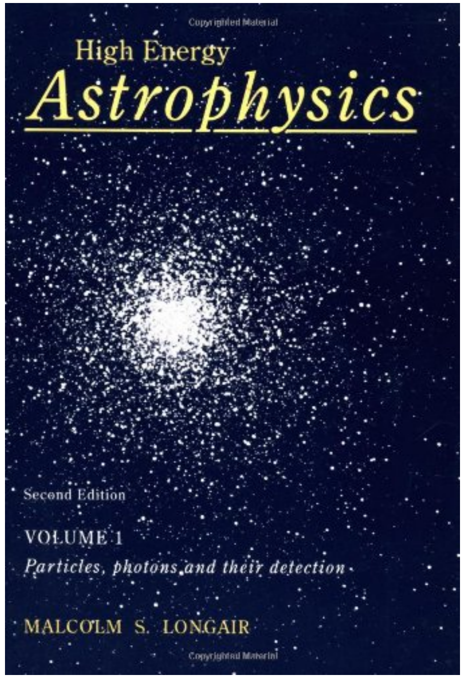

REVIEWS OF MODERN PHYSICS VOLUME 42, NUMBER 2 APRIL 1970

Bremsstrahlung, Synchrotron Radiation, and Compton Scattering of High-Energy Electrons Traversing Dilute Gases

GEORGE R. BLUMENTHAL
Department of Physics, University of California, San Diego, La Jolla, California 92037
ROBERT J. GOULD
*Department of Physics, University of California, San Diego, La Jolla, California 92037** and
School of Physics, University of Sydney, Sydney, N. S. W., Australia 2006

Expressions are derived for the total energy loss and photon-production spectrum by the processes of Compton scattering, bremsstrahlung, and synchrotron radiation from highly relativistic electrons. For Compton scattering, the general case, the Thomson limit, and the extreme Klein–Nishina limit are considered. Bremsstrahlung is treated for the cases where the electron is scattered by a pure Coulomb field and by an atom. For the latter case the effects of shielding are discussed extensively. The synchrotron spectrum is derived for an electron moving in a circular orbit perpendicular to the magnetic field and also for the general case where the electron's motion is helical. The total photon-production spectrum is derived for each process when there is a power-law distribution of electron energies. The problems of the effects of the three processes on the electron distribution itself are considered. It is shown that if the electron loses a small fraction of its energy in a single occurrence of a process, the electron distribution function satisfies a continuity equation which is a differential equation in energy space. For the more general case where the electron can lose energy in discrete amounts (as in bremsstrahlung and extreme Klein–Nishina Compton losses), the electron distribution function satisfies an integro-differential equation. Some approximate solutions to this equation are derived for certain special cases.

CONTENTS

* Permanent address.

1. INTRODUCTION

In a number of areas of astrophysics, for example in considerations of models of cosmic radio sources, problems involving the interaction of a highly relativistic electron with its surrounding medium are common. This "medium" is usually a low-density partially ionized gas with a cosmic element abundance (consisting mostly of hydrogen and helium) which is permeated by a radiation field and a magnetic field. The electron interacts with this medium by means of essentially four processes: (i) by making elastic and inelastic collisions with the atoms and ions of the gas, (ii) by emitting a bremsstrahlung photon during these same scatterings, (iii) by undergoing Compton scatterings with the photons of the radiation field, (iv) by being deflected by the magnetic field, emitting synchrotron radiation or "magnetic bremsstrahlung" in the process. The first process (i) is important only at low energies $\gamma_e = E_e/mc^2 \lesssim 1000$ (cf. GB67) and will not be considered in this review. There are two reasons for treating the other three processes together in a single review. First, all three are photon-producing processes[1] and can therefore be directly responsible for gaining information about the interaction of the electrons with the medium through the detection of these photons. Second, each process is essentially a special case of one basic process; this process is Compton scattering. Bremsstrahlung [process (ii)] can be considered as Compton scattering of the virtual photons of the Coulomb fields of the particles in the scattering system;

[1] The pure Compton-scattering process (iii) does not produce a new photon. However, in collision with a highly relativistic electron, a low-energy photon from the radiation field has its energy increased by a large factor, so that a new *high-energy* photon is produced.

237

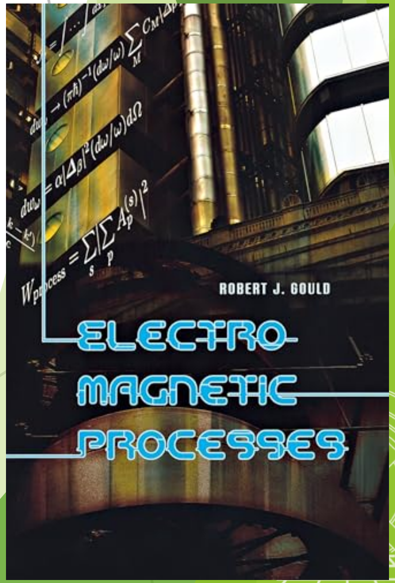

Blumenthal, G.R. & Gould, R.J., Reviews of Modern Physics, vol. 42, Issue 2, pp. 237-271

Where Do X-rays Come From?

- the first observed X-rays from Geiger counters mounted to rockets and balloons after WWII
- first experiments detected the Sun, Sco X-1, CXB

source	mechanism
Solar wind & comets	photoionization and charge exchange
planetary atmospheres and aurorae	fluorescence
stellar/Solar coronae	amalgamation of many mechanisms
supernovae	shocked plasm
accreting compact objects	blackbody
cooling compact objects	? and laboratory astrophysics
collimated jets	synchrotron and scattering
galaxy clusters	thermal Bremsstrahlung

Jonathan will dive more deeply into the various cosmic origins of X-rays in the following presentation.

X-ray Optics

- photons at X-ray energies will not reflect off regular mirrors
- X-rays can reflect off surfaces at shallow angles, referred to as *grazing incidence*
  - analogy: skipping stones across water instead of dropping them straight in
- an incident X-ray photon impacting with a grazing angle θ_i will coherently scatter with the law of reflection, $\varphi_i = \varphi_0$
- modern X-ray telescopes focus photons with grazing angles of $\sim 0.5^\circ$–1°

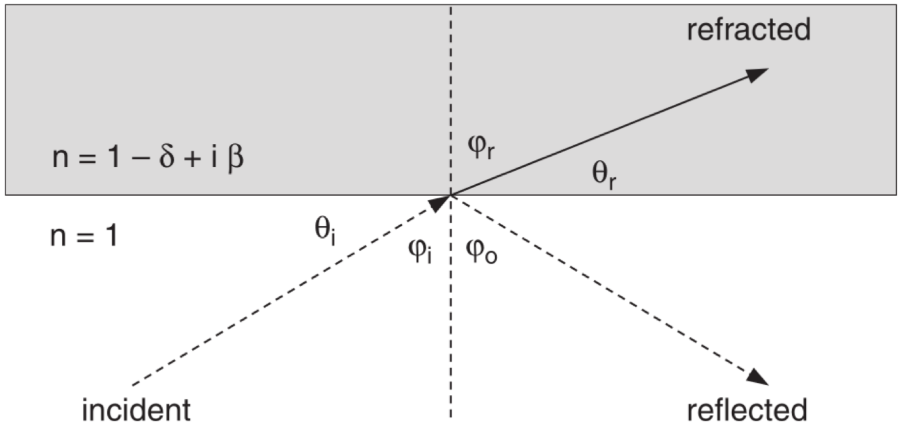

Fig. 1.1 An X-ray in the vacuum (unshaded lower region) impacts a medium (shaded upper region) at a grazing angle θ_i. When the real part of the index of refraction, $1–\delta$, is less than 1, the refracted angle θ_r is smaller than the grazing angle. Since $\cos\theta_r$ cannot be larger than 1, there is total external reflection for grazing angles less than $\arctan(1 - \delta)$

Handbook of X-ray Astronomy, Chapter 1

CHANDRA X-RAY OBSERVATORY

CENTER FOR ASTROPHYSICS HARVARD & SMITHSONIAN

Wolter Type I Mirrors

- paraboloid–hyperboloid pairs
- geometric area of a paraboloid segment:
$$A_{\mathrm{geom}} \approx 2\pi R l \theta_{\mathrm{i}}$$
- reflecting surfaces coated with high-Z metal; reflectivity is a strong function of the incident energy
- assuming there are no support struts, reflective area is the geometric area scaled by R^n, where n is the number of reflective surfaces
- mirror shells can be nested
  - unobstructed effective area is the sum of the reflective areas

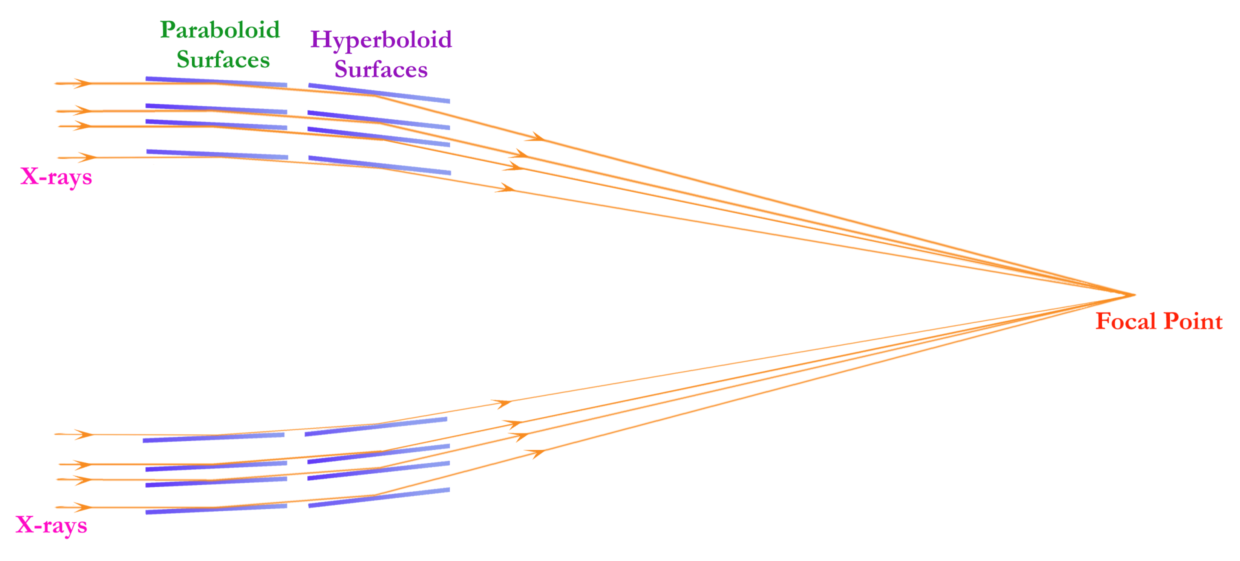

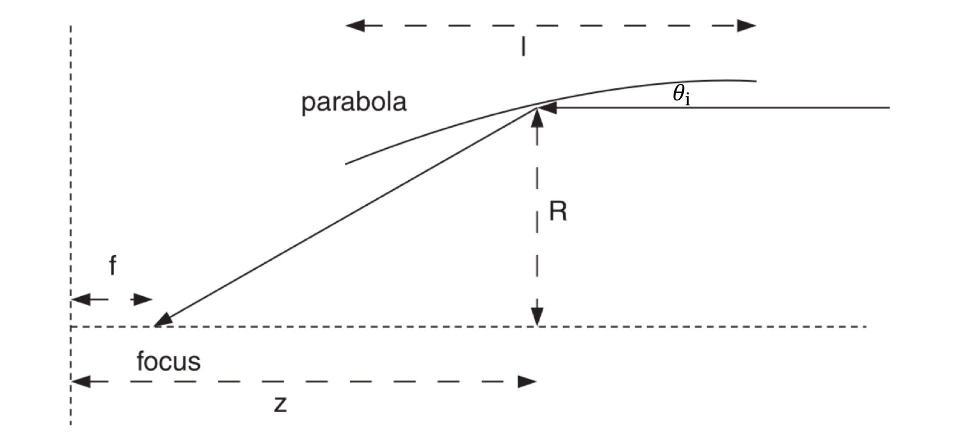

Fig. 1.2 Reflection from a parabolic surface. Rays parallel to the axis are focused at the point f

Handbook of X-ray Astronomy, Chapter 1

Wolter I Off-Axis

- off-axis, effective area falls off and the angular resolution degrades
- PSF morphology distortion is energy dependent

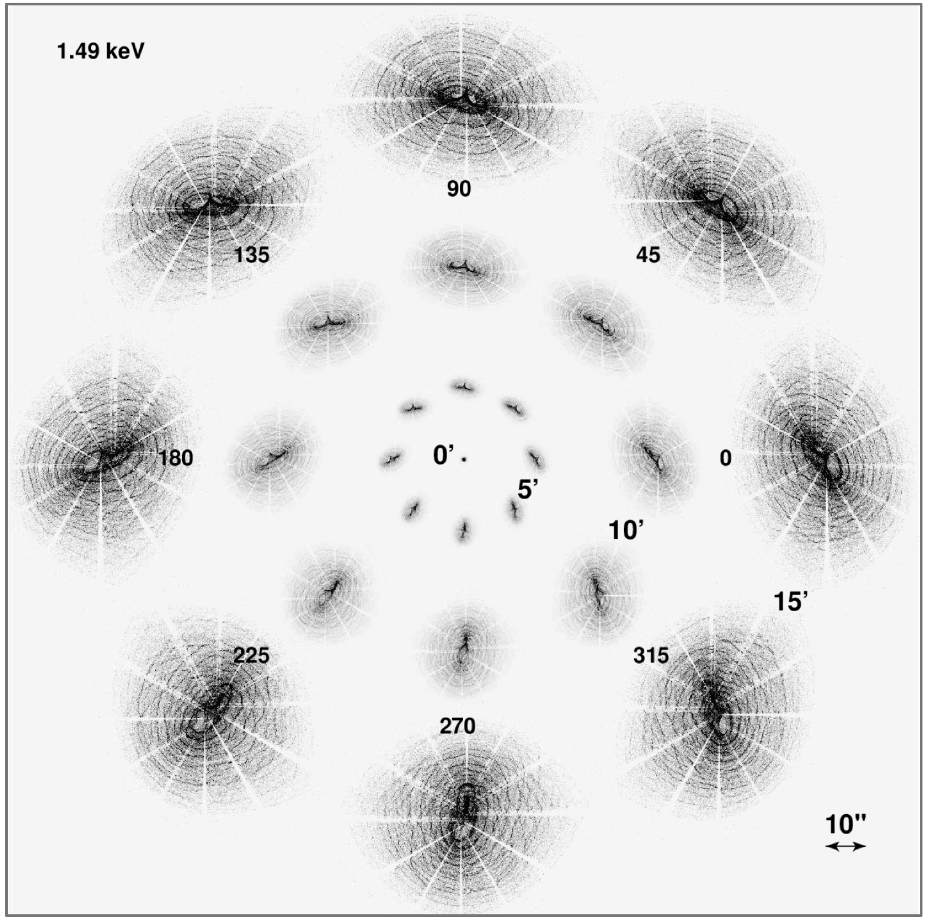

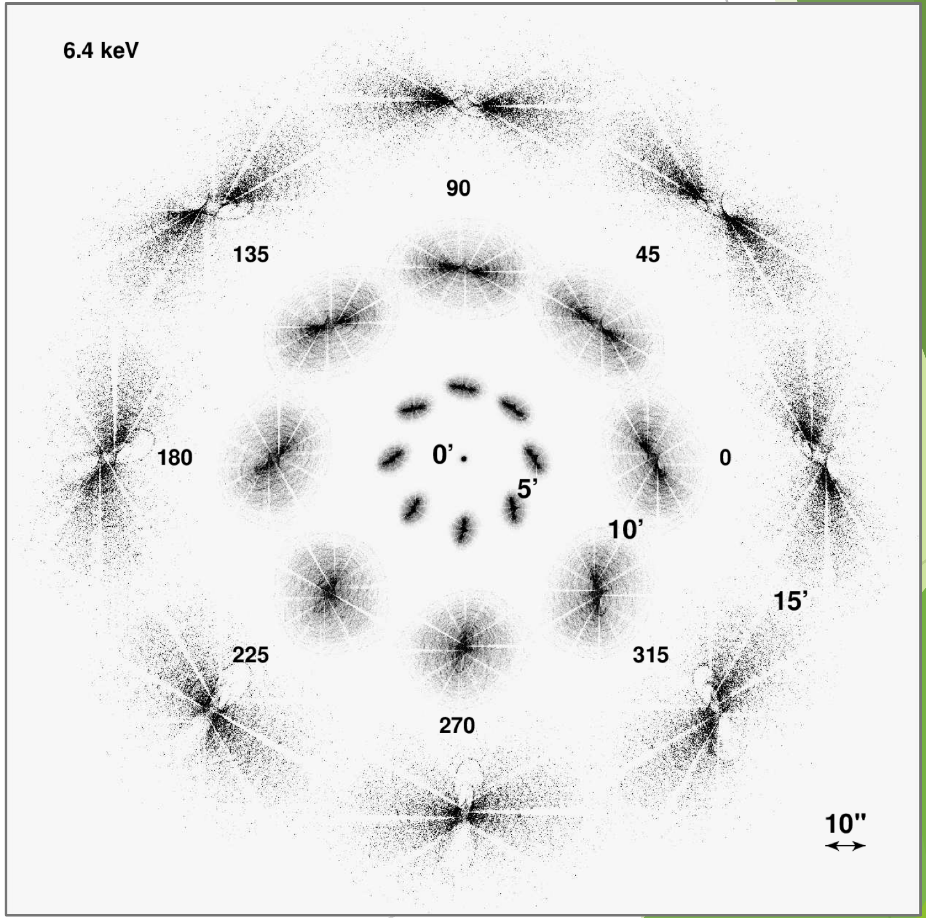

High Resolution Mirror Assembly

HRMA

- four mirror shell pairs fabricated of Zerodur® glass-ceramic
- smoothest surfaces ever figured; mirrors ground to a tolerance < 4 Å
  - XRCF measurements indicate that HRMA figured to provide a PSF $< 0.2''$ FWHM

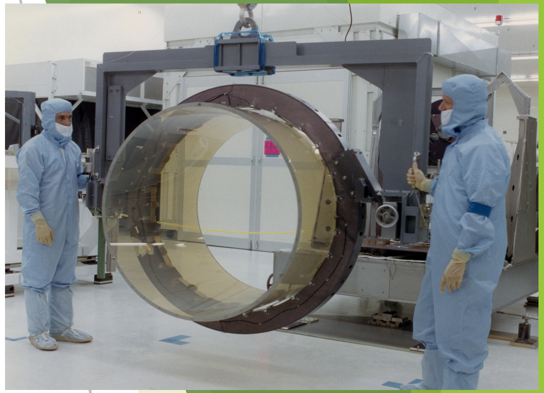

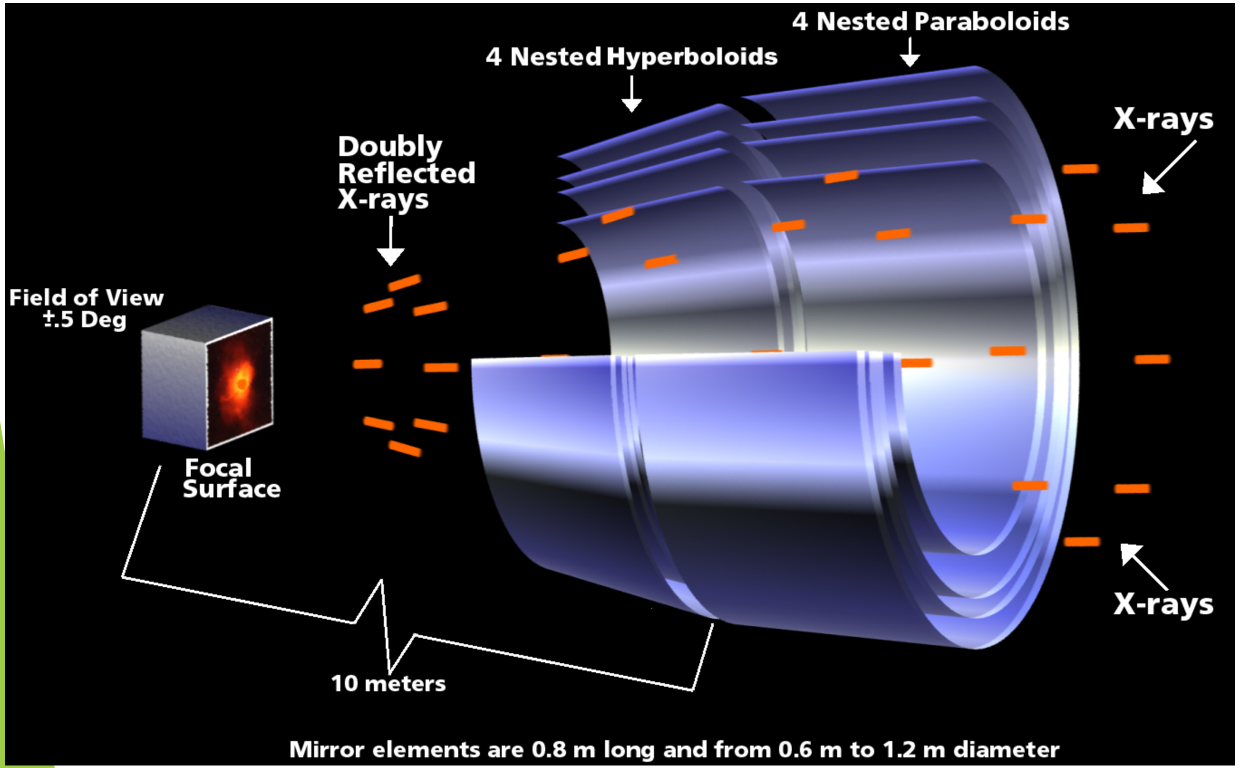

High angular resolution is dependent on the smoothness of the reflecting surface and the concentric alignment of the mirror shells. Surface roughness greater than the wavelength of the photons will cause scattering and broaden the PSF.

HRMA continued…

- shell thickness varies between 1.6–2.4 cm, with thicker walls for the outer shells
- the roughness of the mirror pairs vary, with MP1 being the roughest and MP6 the smoothest
- rougher surfaces tend to scatter higher energy photons more than lower energy ones, thus broadening the PSF at higher energies
- the nested nature of the HRMA mirrors, each pair has a different mean grazing angle, ranging from 50.6′ for MP1 to 26.7′ for MP6
  - lower-energy photons better focused by outer MP shells
  - higher-energy photons best focused by inner MP shells

CHANDRA X-RAY OBSERVATORY

Chandra HRMA Characteristics

Optics	Wolter Type-I
Mirror coating	Iridium (330 Å, nominal)
Mirror outer diameters (1, 3, 4, 6)	1.23, 0.99, 0.87, 0.65 m
Mirror lengths (P_n or H_n)	84 cm
Total length (pre- to post-collimator)	276 cm
Unobscured clear aperture	1145 cm^2
Mass	1484 kg
Focal length	10.070 ±0.003 m
Plate scale	48.82 ±0.02 μm $arcsec^{-1}$
Exit cone angles from each hyperboloid:	
θ_c (1, 3, 4, 6)	3.42°, 2.75°, 2.42°, 1.80°
θ_d (1, 3, 4, 6)	3.50°, 2.82°, 2.49°, 1.90°
f-ratios (1, 3, 4, 6)	8.4, 10.4, 11.8, 15.7
PSF FWHM (with detector)	< 0.5 arcsec
Effective area:	@ 0.25 keV 800 cm^2 @ 5.0 keV 400 cm^2 @ 8.0 keV 100 cm^2
Ghost-free field of view	30 arcmin diameter

Proposers' Observatory Guide, Table 4.1

HRMA continued…

- coated with 330 Å layer of iridium via sputtering
  - chromium binding substrate
  - XRCF PSF measurement < 0.25″ FWHM

- reflectivity exhibits atomic edge features of mirror materials

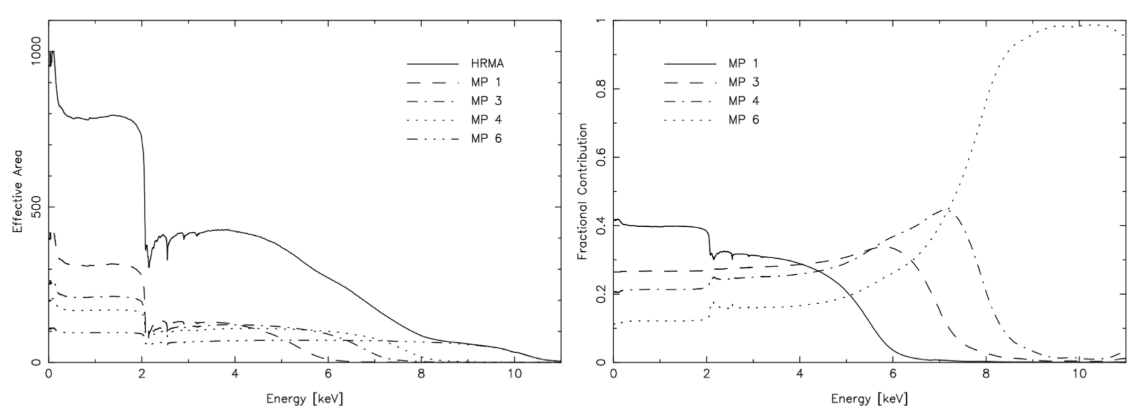

(a) HRMA effective area and individual shell effective areas

(b) Fractional contribution of the four mirror pairs to the overall HRMA effective area.

The HRMA User's Guide, Fig. 3

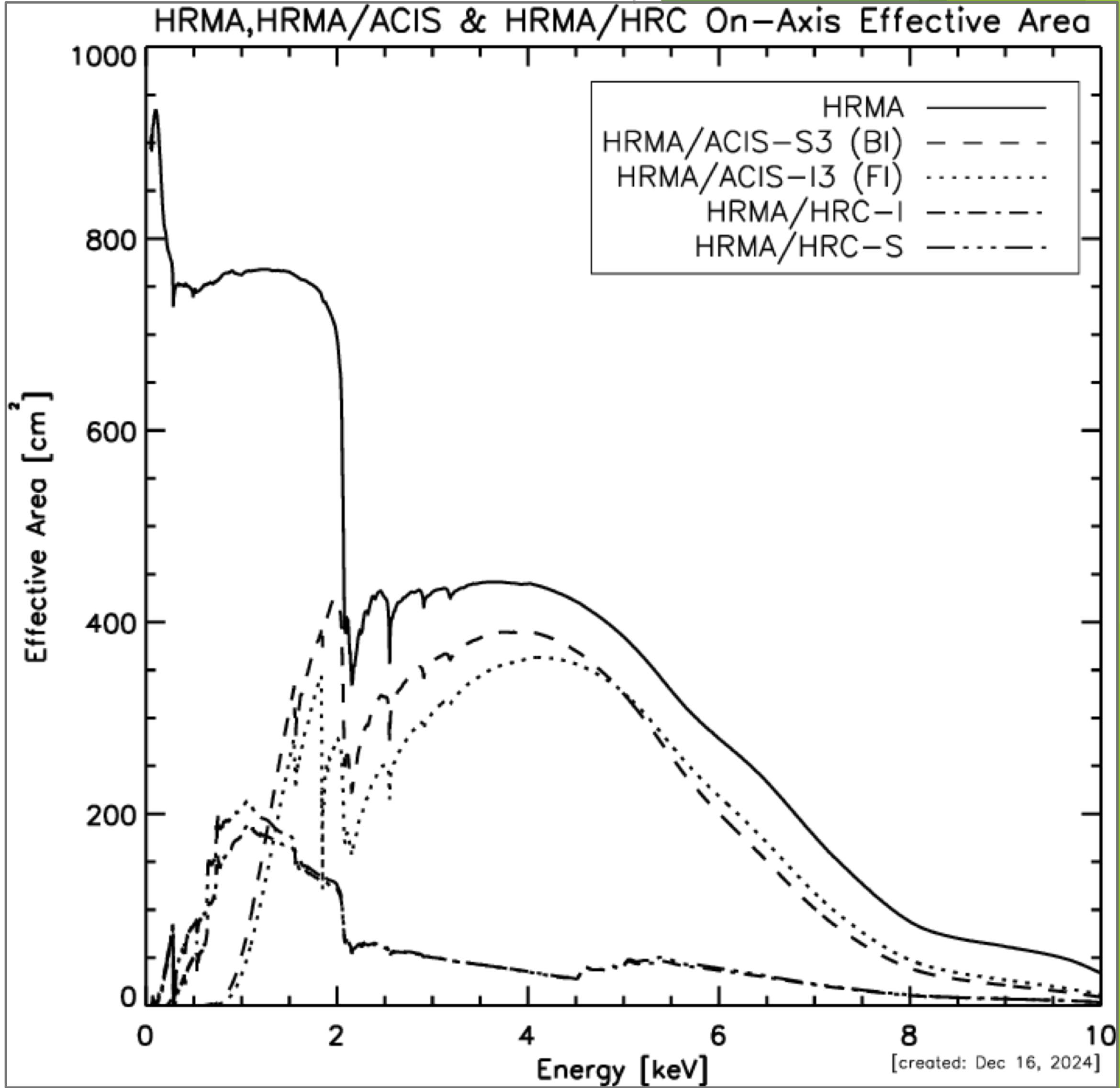

Comparing X-ray Telescope Observations

CHANDRA
X-RAY OBSERVATORY

Orion Open Star Cluster

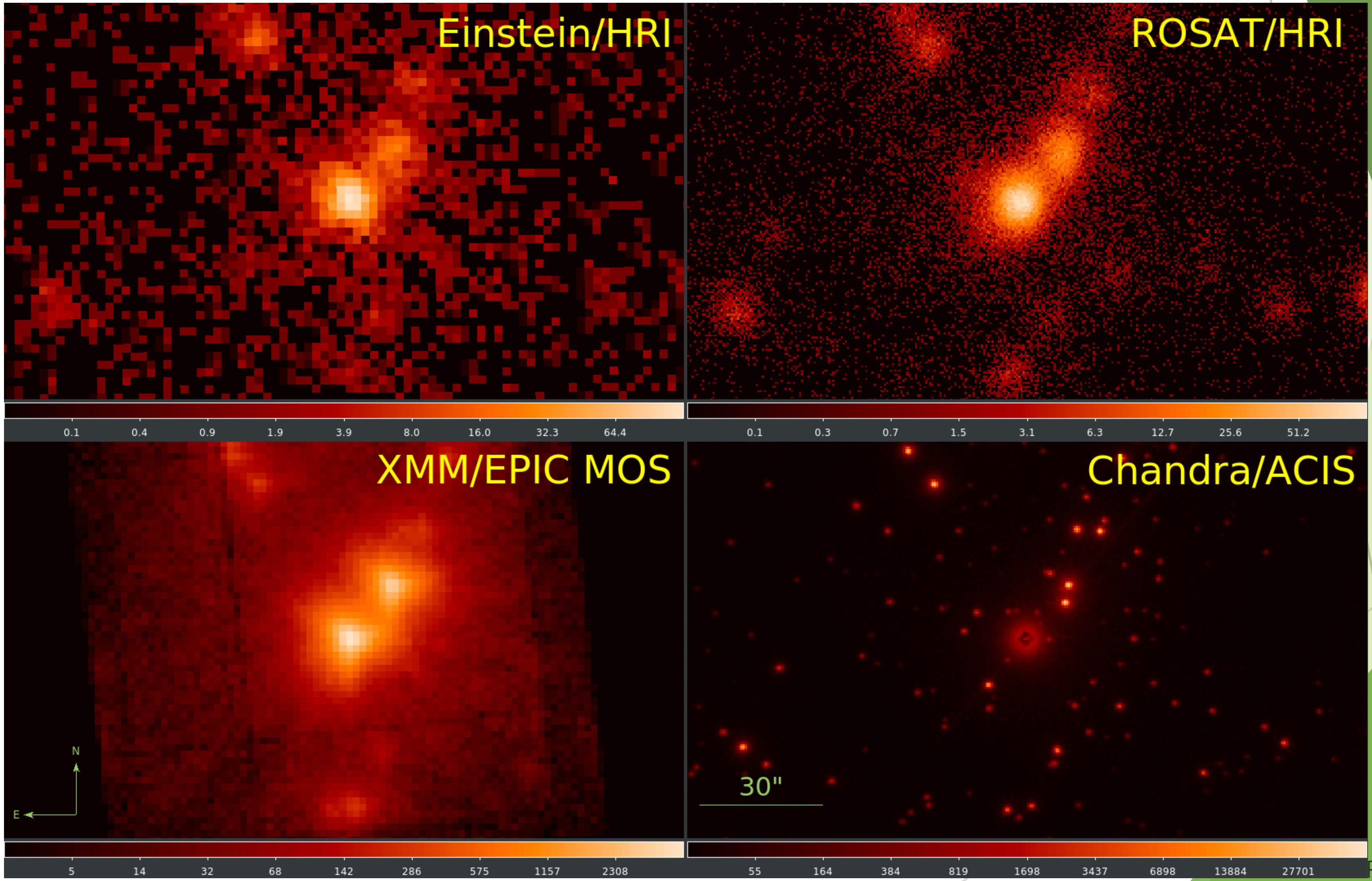

R FOR ASTROPHYSICS
HARVARD & SMITHSONIAN

Comparing X-ray Telescope Observations

Cassiopeia A

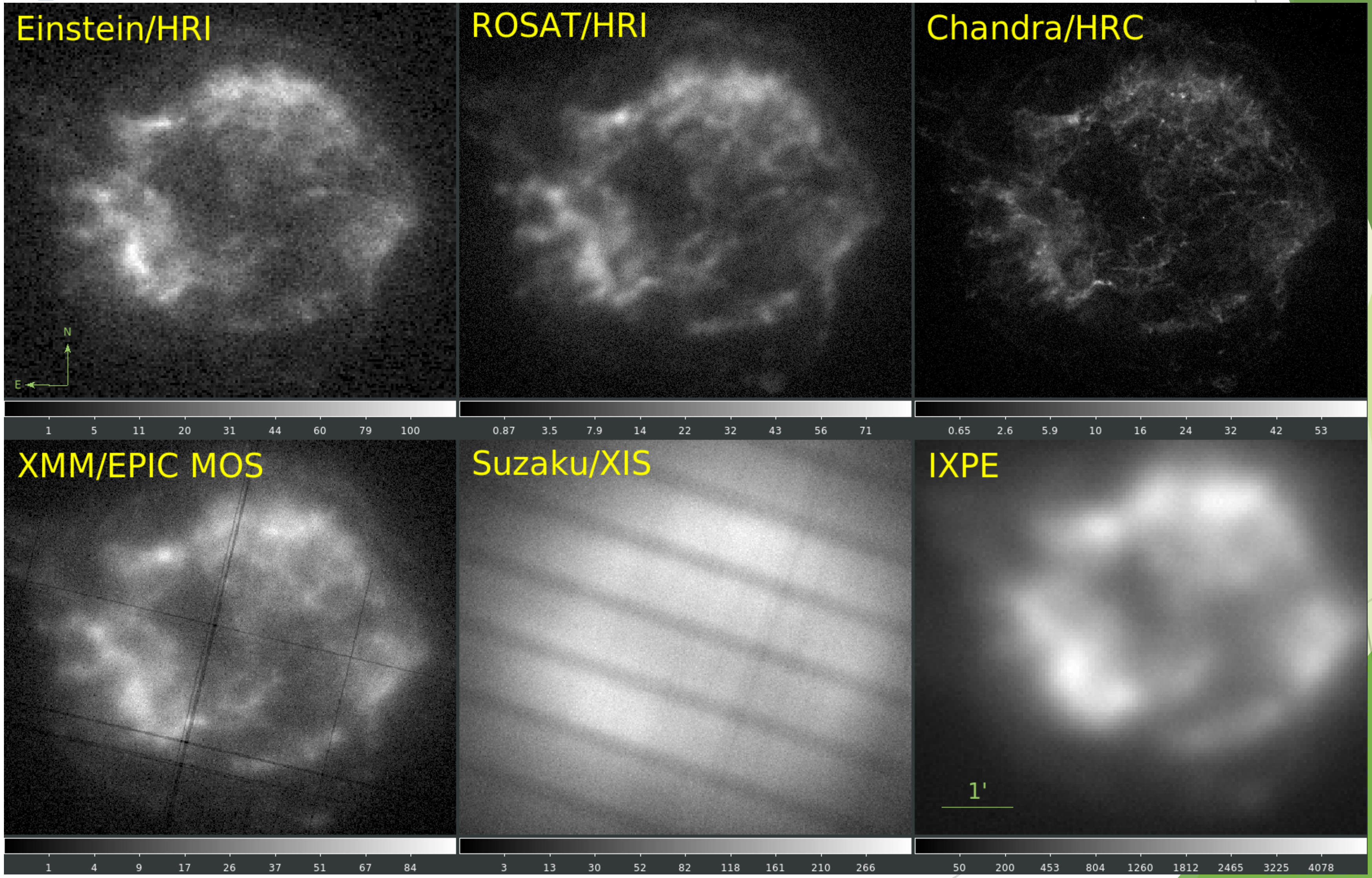

CHANDRA
X-RAY OBSERVATORY

Consequences of High Spatial Resolution

- separate out point sources in crowded fields
- higher sensitivity to faint objects
- resolving diffuse, fine structure

CENTER FOR ASTROPHYSICS
HARVARD & SMITHSONIAN

HRMA PSF Artifact

A feature within the central arcsecond of the HRMA point spread function has been observed on both HRC and ACIS. The PSF artifact lies 0.6-0.8 arcsec off-axis, and appears fixed relative to detector coordinates. It but does not affect images on scales larger than one arcsecond.

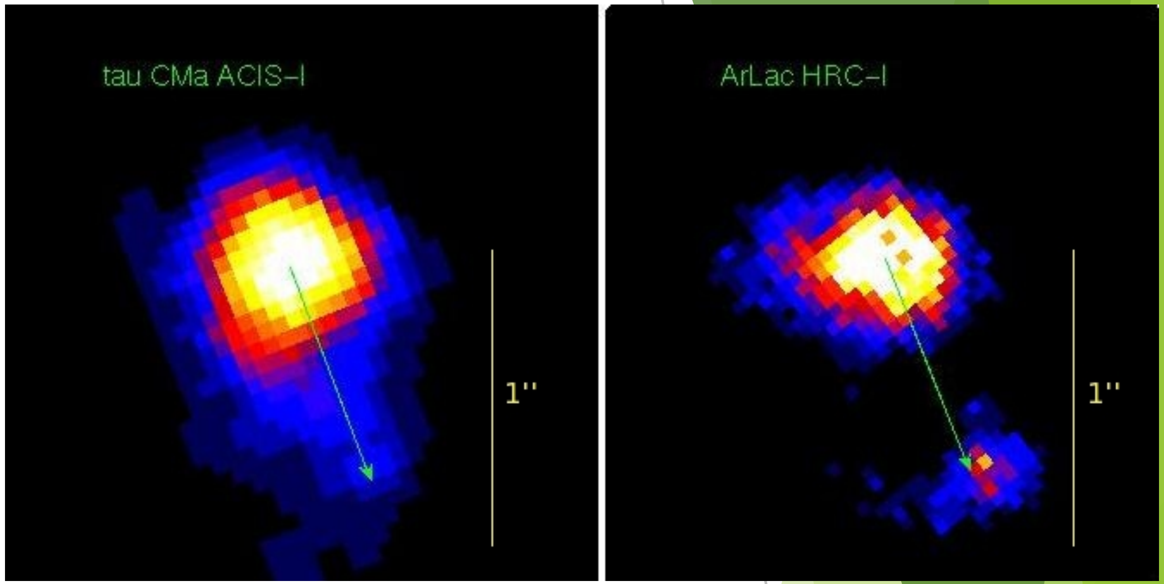

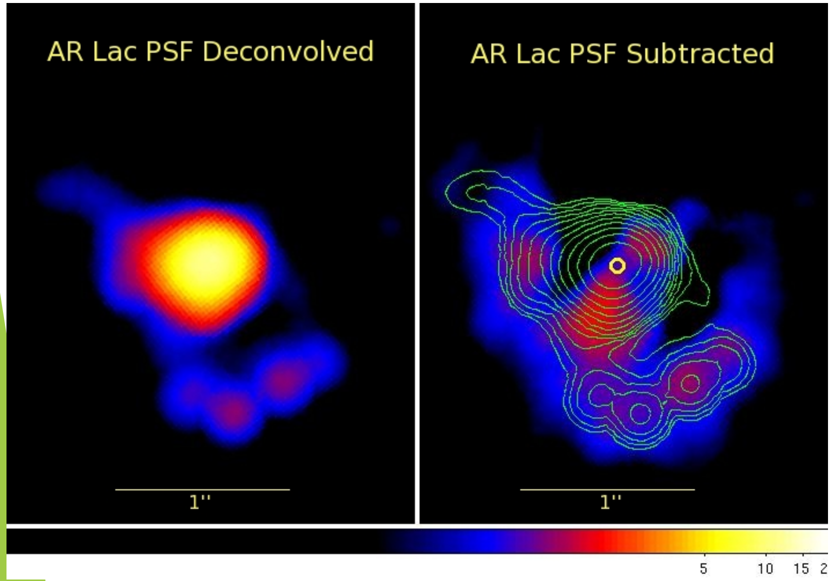

The feature's brightness is ~5% of the total brightness and appears as a hook-like structure and has been observed since early on the mission.

Chandra X-ray Observatory

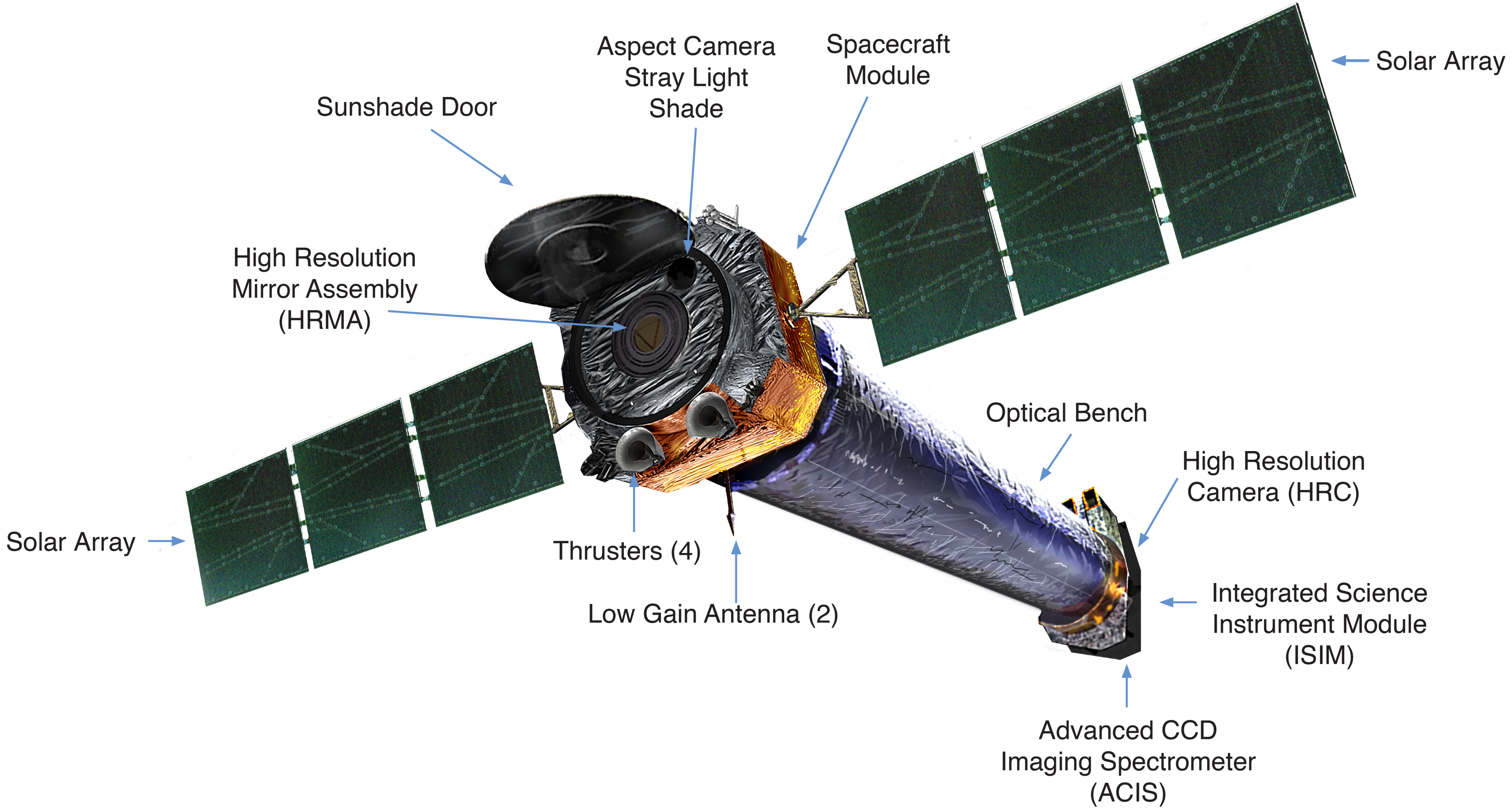

CHANDRA X-RAY OBSERVATORY

CENTER FOR ASTROPHYSICS HARVARD & SMITHSONIAN

Deployment

- launched aboard *Columbia* (STS-93) on July 23, 1999
- heaviest payload ever launched by a space shuttle
- while a bit shorter in length than *HST*, *Chandra* was deployed with a rocket attached, which made it the longest payload unit deployed by a space shuttle

Deployment

- inserted into highly elliptical Earth orbit
  - Inertial Upper Stage — 2 burns; jettisoned
  - Integral Propulsion System — 5 burns; disabled

- deployed with 50 years of consumables

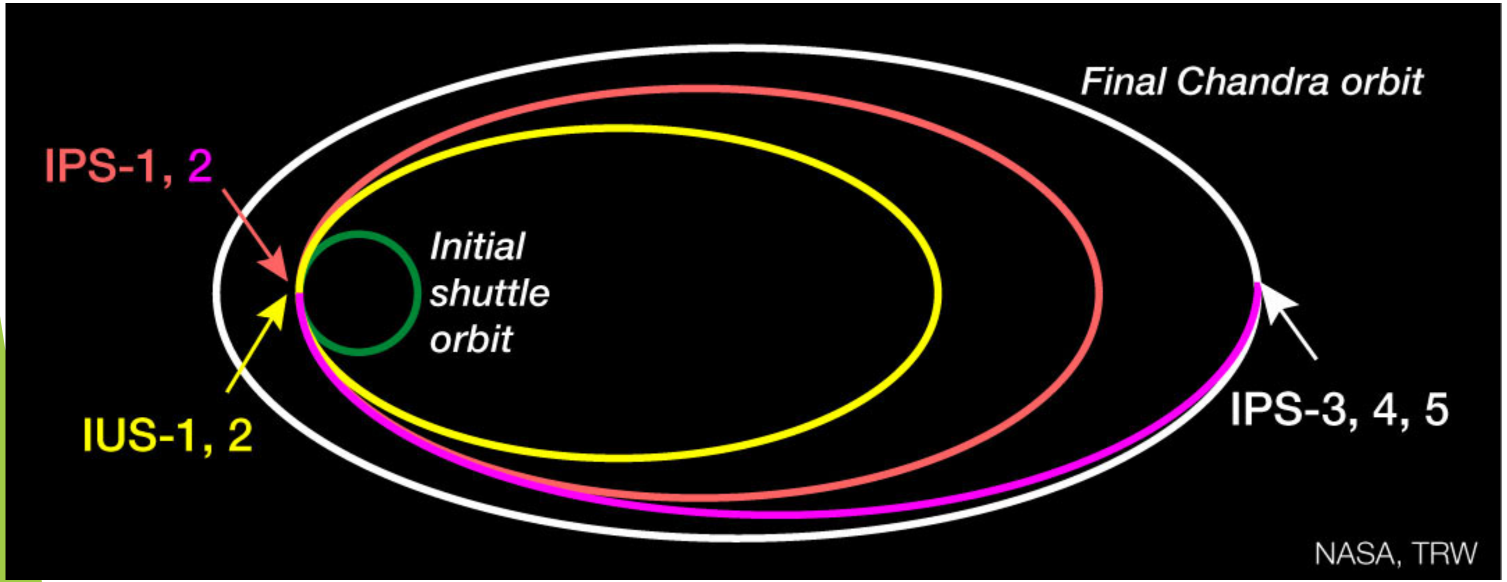

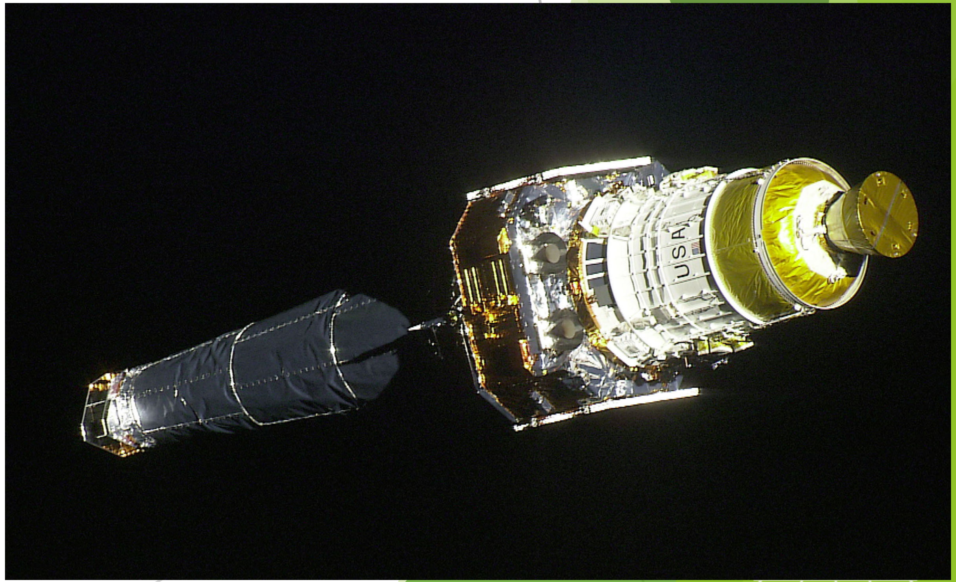

Chandra Orbit

- highly elliptical orbit (July 2023, POG 1.8)
  - perigee: 1,045 km
  - apogee: 147,400 km
  - eccentricity: 0.91
- ~63.5 hours (229 ksec)
- radiation belt passage approaching perigee results in ~25% of orbit being unusable
- observing efficiency: ~70%

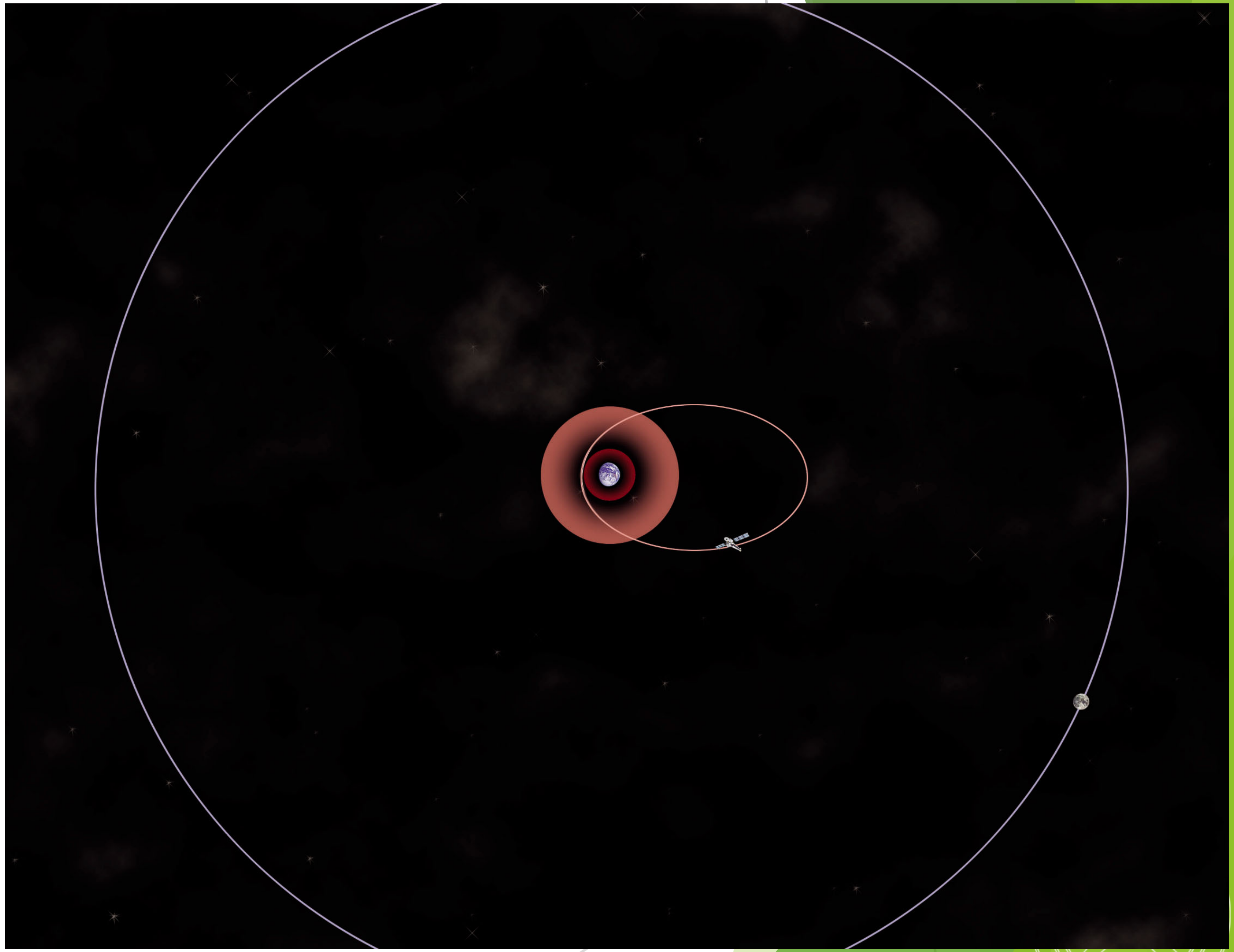

Pointing and Star Tracking

- Pointing Control and Aspect Determination (PCAD)
  - two Inertial Reference Units with two gyroscopes each provide spacecraft attitude and orientation information
  - Reaction Wheel Assembly with six reaction wheels used to maintain pointing and maneuver; used in concert with IRUs to determine wheel rotation rate
  - Momentum Unloading Propulsion System (MUPS) unloads momentum built-up in RWA with reaction thrusters while reaction wheels spin down
  - Aspect Camera Assembly (ACA), 11.2 cm 11.2 cm Ritchey-Chretien telescope for guide star tracking to determine pointing
- star tracker has 8 observing slots; typically using 3 fiducial lights and 5 guide stars

Pointing and Star Tracking

- pointing accuracy decreased with time due to higher temperatures
  - absolute pointing of 0.8 arcsec as of 2022
  - absolute pointing accuracy was 0.6 arcsec, pre-2022
- ACA can be used for optical photometry by dropping a guide star
  - limited to source with $m_{\mathrm{ACA}} \approx 10.3–5.2$
  - degradation of the image reconstruction and celestial location accuracy

Dither

Rather than locking and holding its pointing on a target *Chandra* dithers about its pointing position in a Lissajous pattern to average across calibration uncertainties.

- for ACIS, dithering keeps one bad pixel from ruining an entire observation and smooths over chip gaps
- for HRC, it prevents too many photons from entering a single microchannel plate pore

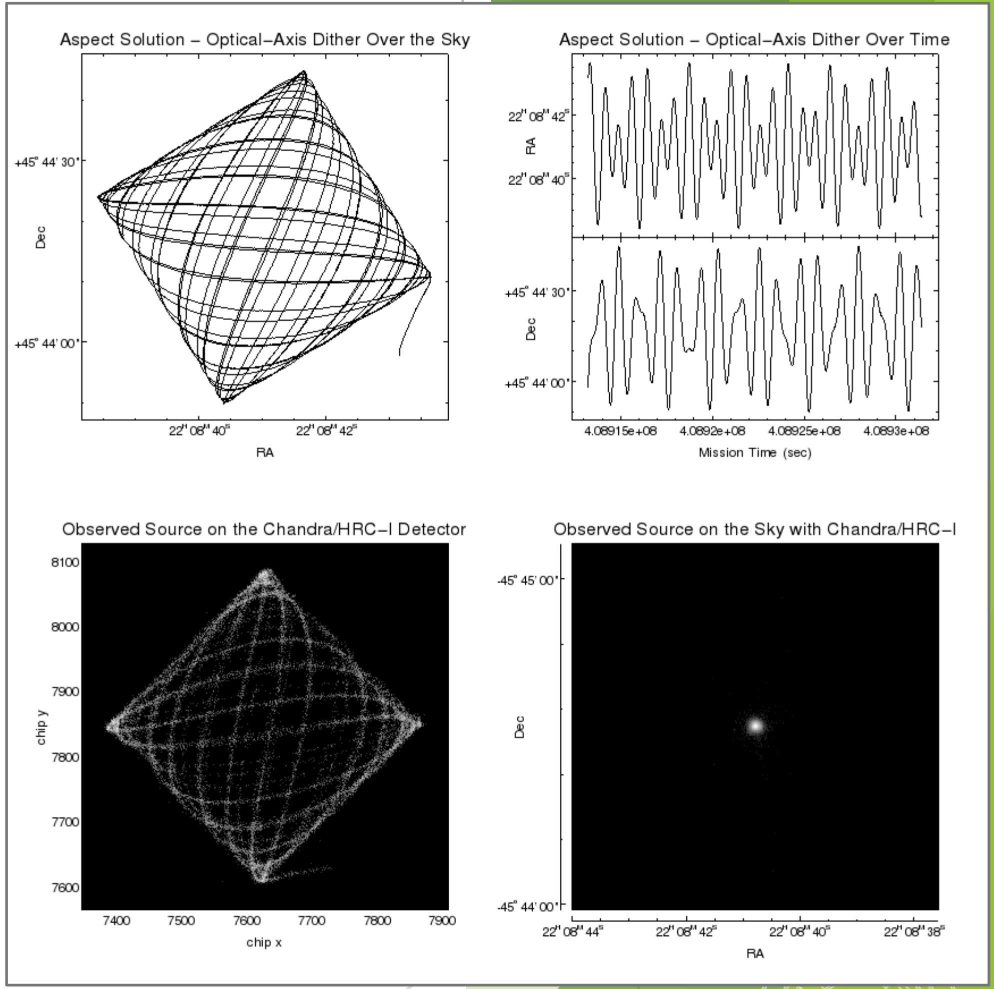

Detector	Peak-to-peak Span (arcsec)	Nominal Period Yaw (s)	Nominal Period Pitch (s)
ACIS before October 2022	16	1000.0	707.1
ACIS starting in October 2022	32	2000.0	1414.0
HRC	40	1087.0	768.6

Dither
continued…

- dithering also smooths out the small effects of spatial detector QE variations

- photons will land on different parts of the detector during an observation but an ‘undithered’ image may be reconstructed using the arrival time of each photon alongside the housekeeping data from the aspect camera

- reconstructed position accuracy typically $\lesssim 0.6''$ but has varied over the course of the mission

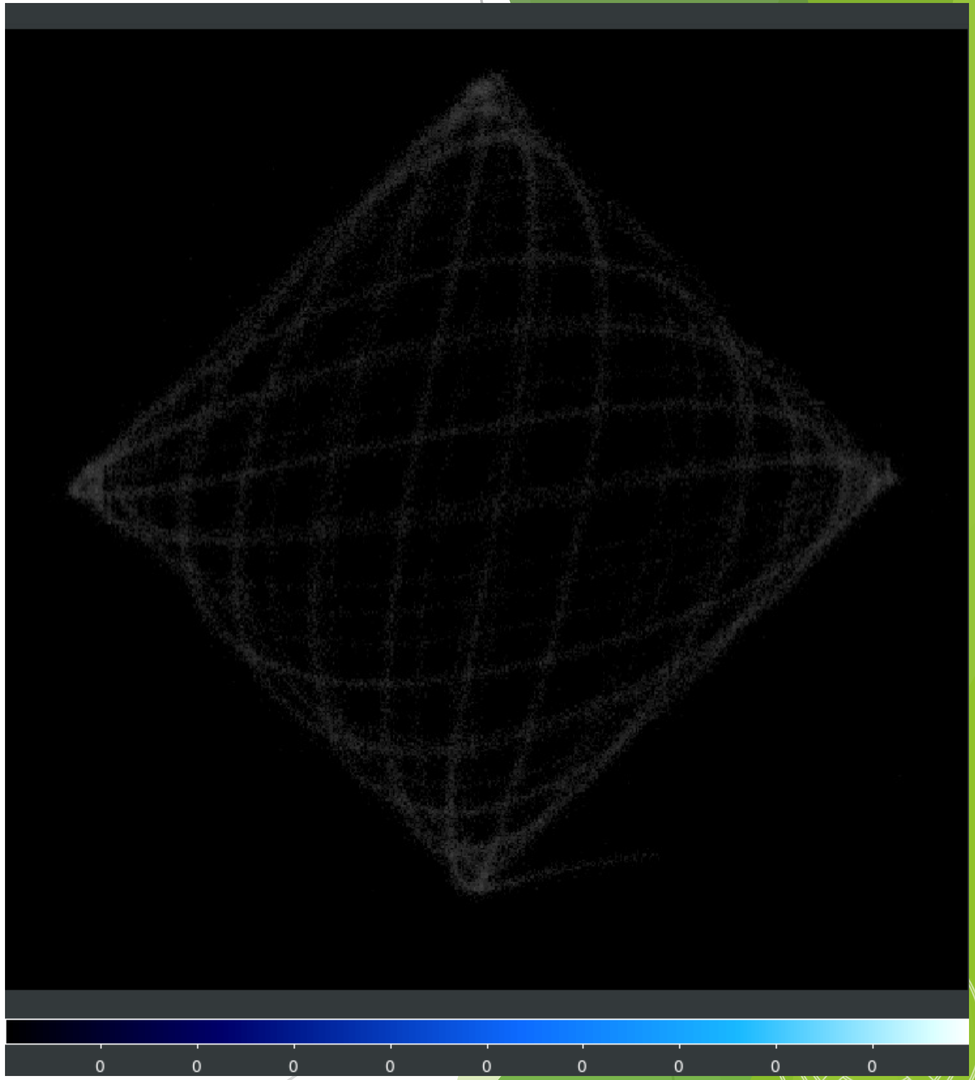

ObsID 13182: AR Lac
HRC-I 18 ksec, 20 sec time bins

Phoning Home

Uplink/Downlink

- two S-band, low-gain antennae used to communicate with the Deep Space Network (DSN)
- ground-contact can be anywhere between 1–3 times in a 24 hour period for 45–75 minutes
  - the spacecraft typically in contact with the DSN twice daily for an hour per linkup
- during normal science operations, telemetry data are generated on the Observatory at a rate of 32 kbps
  - of which 24 kbps are devoted to the "science stream" data from one of the focal-plane instruments
  - remainder allocated to other spacecraft systems including 0.5 kbps for ‘next-in-line’ instrument
- The data are recorded on one of two solid state recorders each having a capacity of 1.8 Gbits

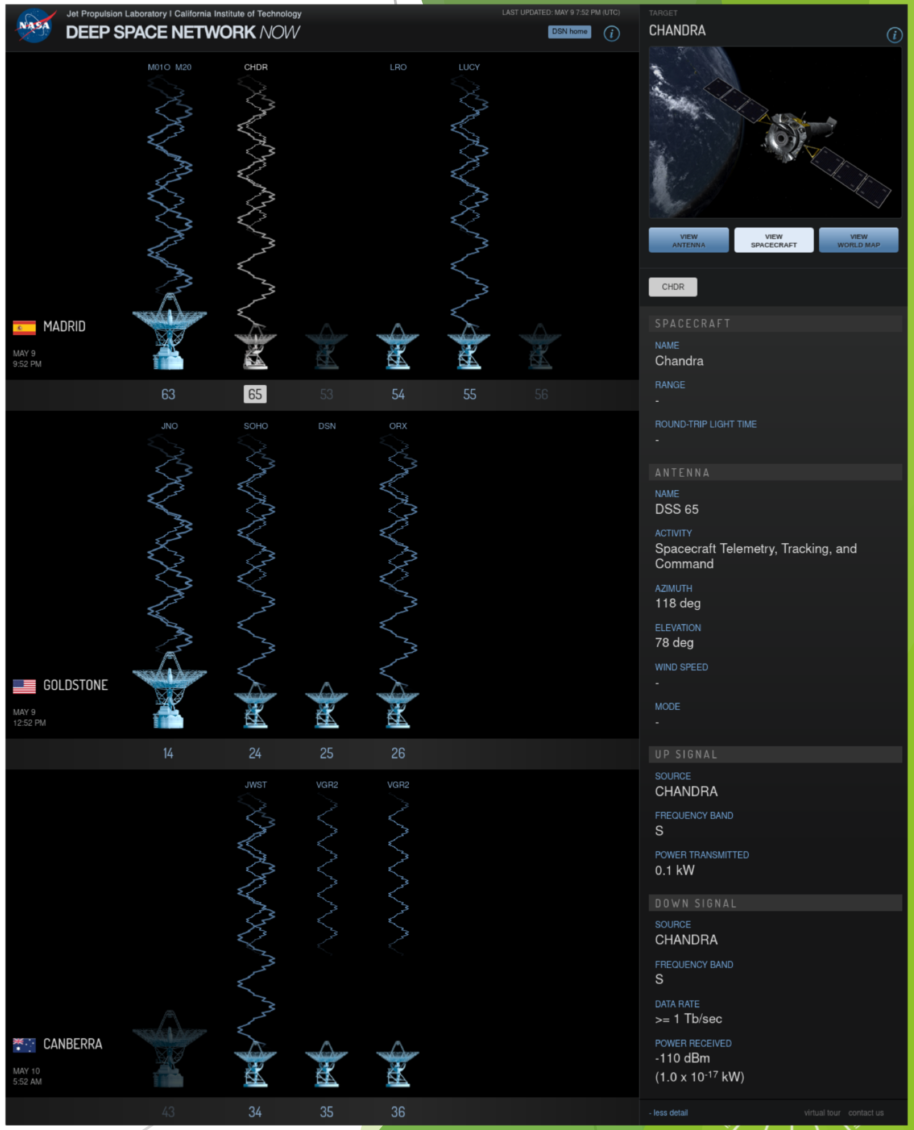

Coordinate Systems

- two primary classes of coordinate systems: sky and detector
  - sky — event position on a fictitious plane tangent to a nominal, fixed celestial pointing direction. This is a linear coordinate system that can be transformed into celestial coordinates.
  - chip — gives row and column number on each CCD or plate
  - det (detector) — a projection of the photon positions onto the tangent plane to the unit sphere, with the tangent point being the telescope's optical axis
  - tdet (tiled detector) —for visualization purposes only; see all the chips placed next to each other but the offsets between the chips are arbitrary
- special coordinates for gratings
- MSC (mirror spherical coordinates) — gives the off-axis angle and azimuth of an event in a fixed frame with respect to the HRMA optical-axis
- the relationship between Sky, Mirrors, & Detectors is called the ***aspect solution***

Chandra Instruments

- Advanced* CCD Imaging Spectrometer (ACIS)
- High Resolution Camera (HRC)
- Electron, Proton, Helium Instrument (EPHIN)
  - defunct particle detector used to monitor the local charged particle environment to protect the focal-plane instruments from particle radiation damage.
  - role superseded by HRC in late 2013, shutdown in 2018
- High-Energy Transmission Grating Spectrometer (HETGS)
- Low-Energy Transmission Grating Spectrometer (LETGS)

*originally 'AXAF' CCD Imaging Spectrometer

Advanced CCD Imaging Spectrometer ACIS

CHANDRA
X-RAY OBSERVATORY

POG Table 6.2: ACIS Characteristics

Focal-plane arrays:	
I-array	4 CCDs placed tangent to the focal surface
S-array	6 CCDs in a linear array tangent to the grating Rowland circle
CCD format	1024 by 1024 pixels
Pixel size	23.985 microns (0.4920±0.0001 arcsec)
Array size	16.9 by 16.9 arcmin ACIS-I
	8.4 by 51.1 arcmin ACIS-S
On-axis effective Area (Cycle 1)	110 cm^2 @ 0.5 keV (FI)
(integrated over the PSF	600 cm^2 @ 1.5 keV (FI)
to > 99% encircled energy)	40 cm^2 @ 8.0 keV (FI)
Quantum efficiency[f]	
Front-illuminated CCD	> 80% between 3.0 and 6.5 keV
	> 30% between 0.7 and 11.0 keV
Back-illuminated CCD	> 80% between 0.8 and 5.5 keV
	> 30% between 0.4 and 10.0 keV
Charge transfer inefficiency (Cycle 1):	
(parallel)	FI: $\sim 2\times10^{-4}$; BI: $\sim 2\times10^{-5}$
(serial)	S3(BI): $\sim 7\times10^{-5}$; S1(BI): $\sim 1.5\times10^{-4}$;
	FI: $< 2\times10^{-5}$
System noise	<~2 electrons (RMS) per pixel

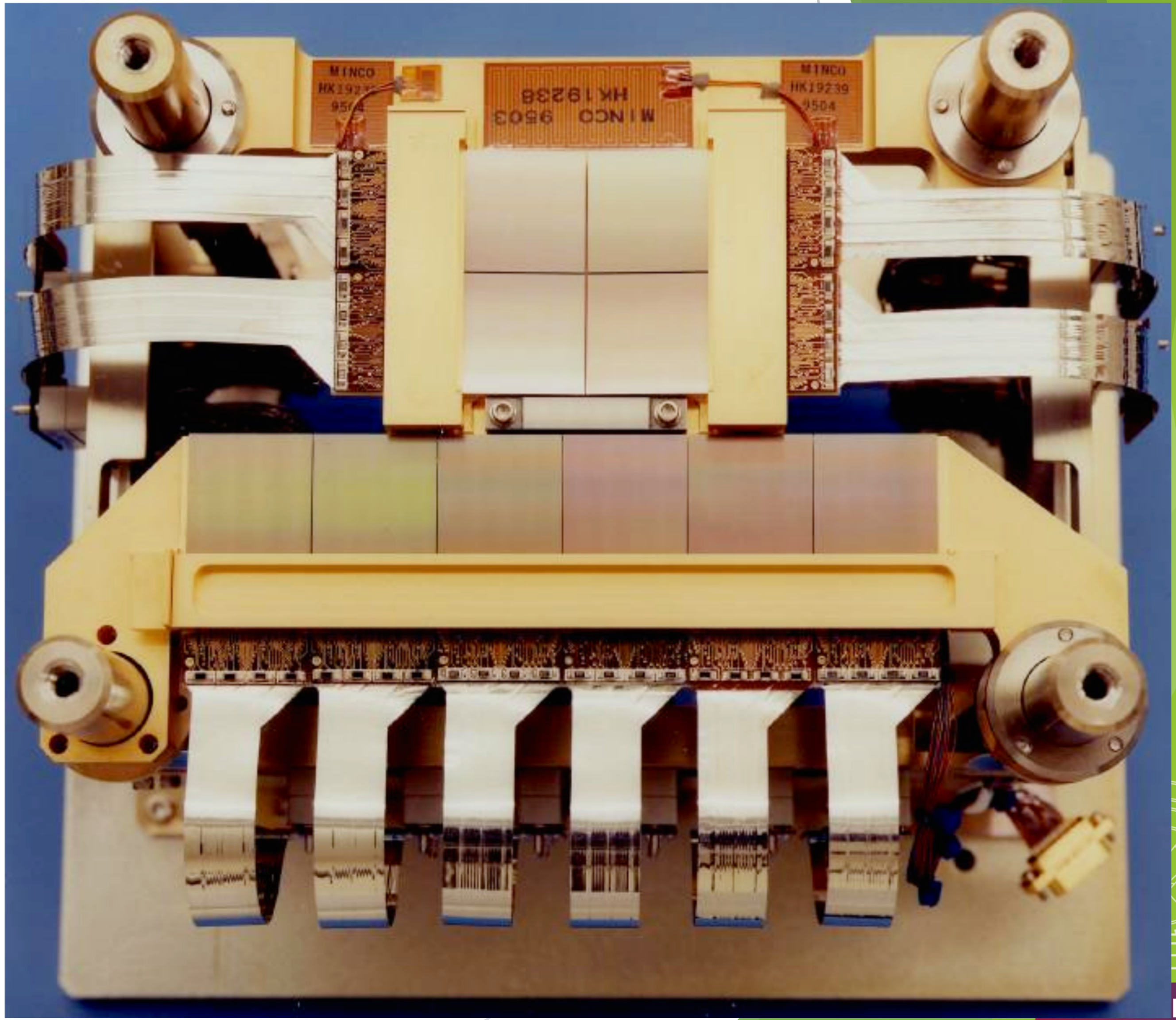

CHANDRA
X-RAY OBSERVATORY

Chip Tilts

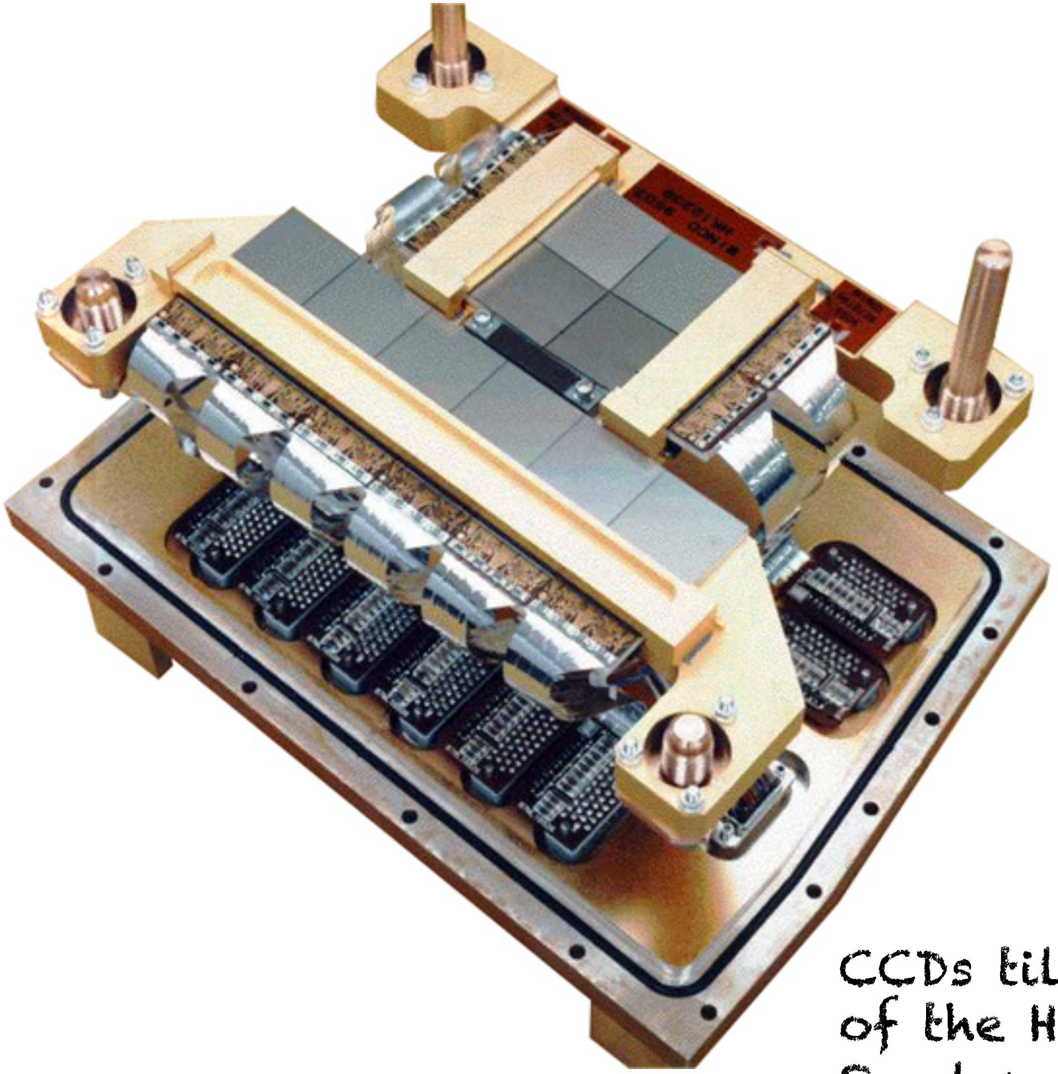

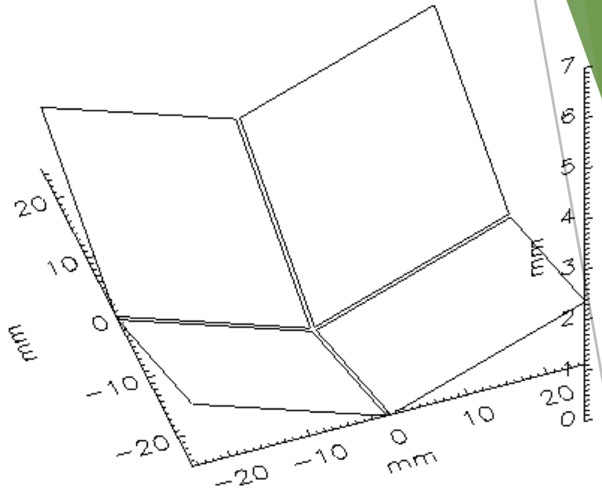

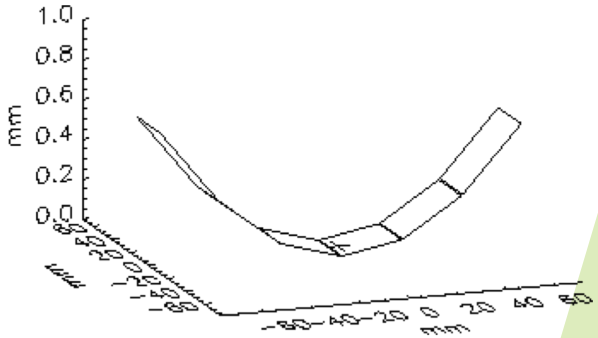

CCDs tilted roughly tracing the paraboloid of the HRMA focal surface (ACIS-I) and Rowland circle used by HETG (ACIS-S)

CENTER FOR ASTROPHYSICS
HARVARD & SMITHSONIAN

CHANDRA X-RAY OBSERVATORY

Charge Coupled Devices

- CCDs are arrays of linked (e.g. coupled) capacitors
  - basic structure
    - a metallic capacitor “gate” structure composing the sensor pixel—ACIS uses MOS capacitors
    - an insulator layer
    - a photosensitive semiconductor (depletion) layer, typically silicon, that can photoelectrically absorb a photon
  - the capacitors hold the electron charge in a series of coupled electron wells that are moved to a discrete well that is systematically read-out as charge
- when a photon is absorbed in the silicon of a CCD, a charge cloud of electron hole pairs is formed (~3.65 eV per pair); the number of electrons hole pairs liberated is linearly proportional to the incident energy
- the pulse-height is a measure of the number of pairs in the cloud and has to exceed a set threshold to be considered as a photon event

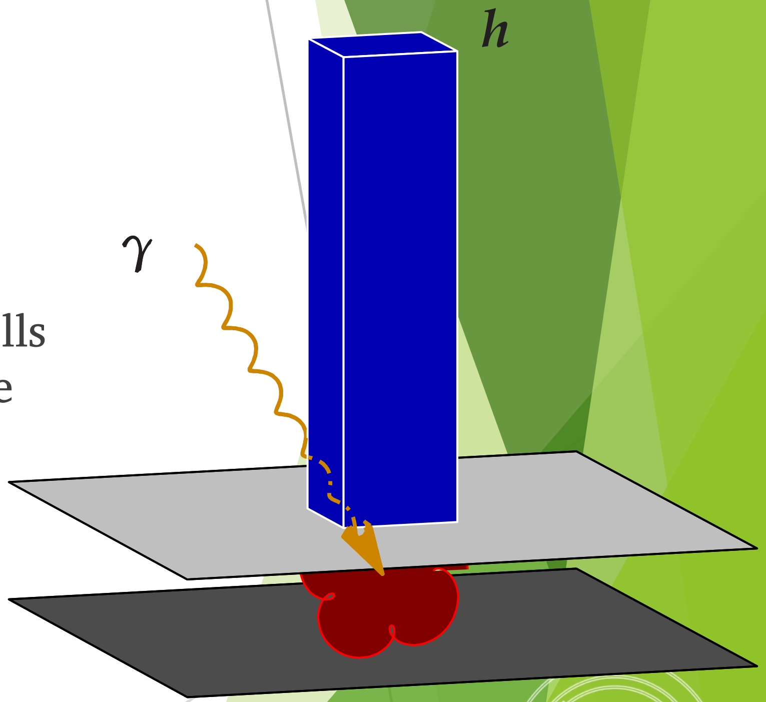

Event Grades

- charge cloud is not necessarily confined to a single pixel ("split events")
- for each event, record position, time, and pulse heights of event island (3×3 pixels for ACIS)
  - the position location is the central pixel of the event island which has the maximum pulse height locally
- events are assigned a grade which characterizes the morphology of the pulse heights in the event island
- "bad" grades more likely to be background (cosmic rays)

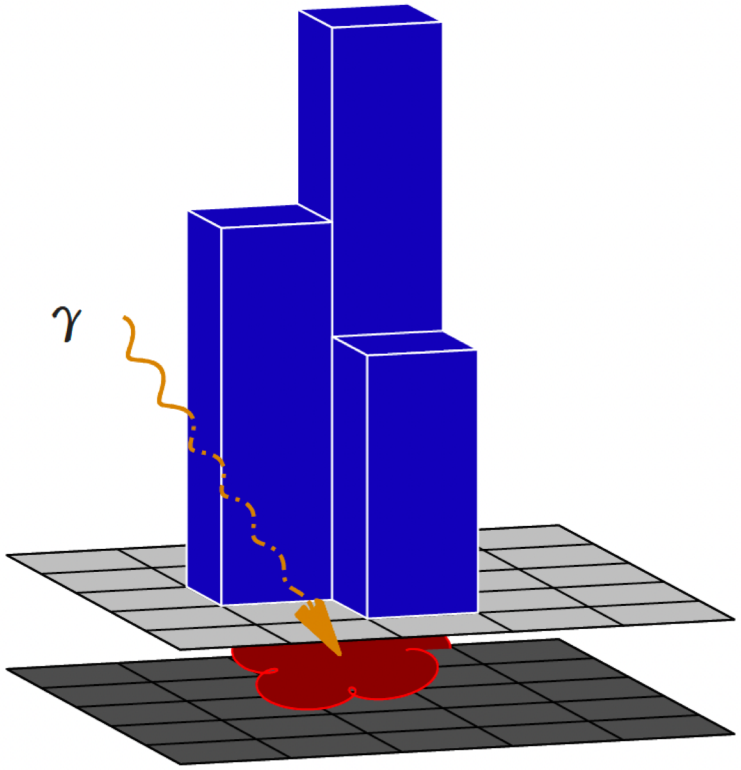

ACIS Event Grades

CHANDRA X-RAY OBSERVATORY

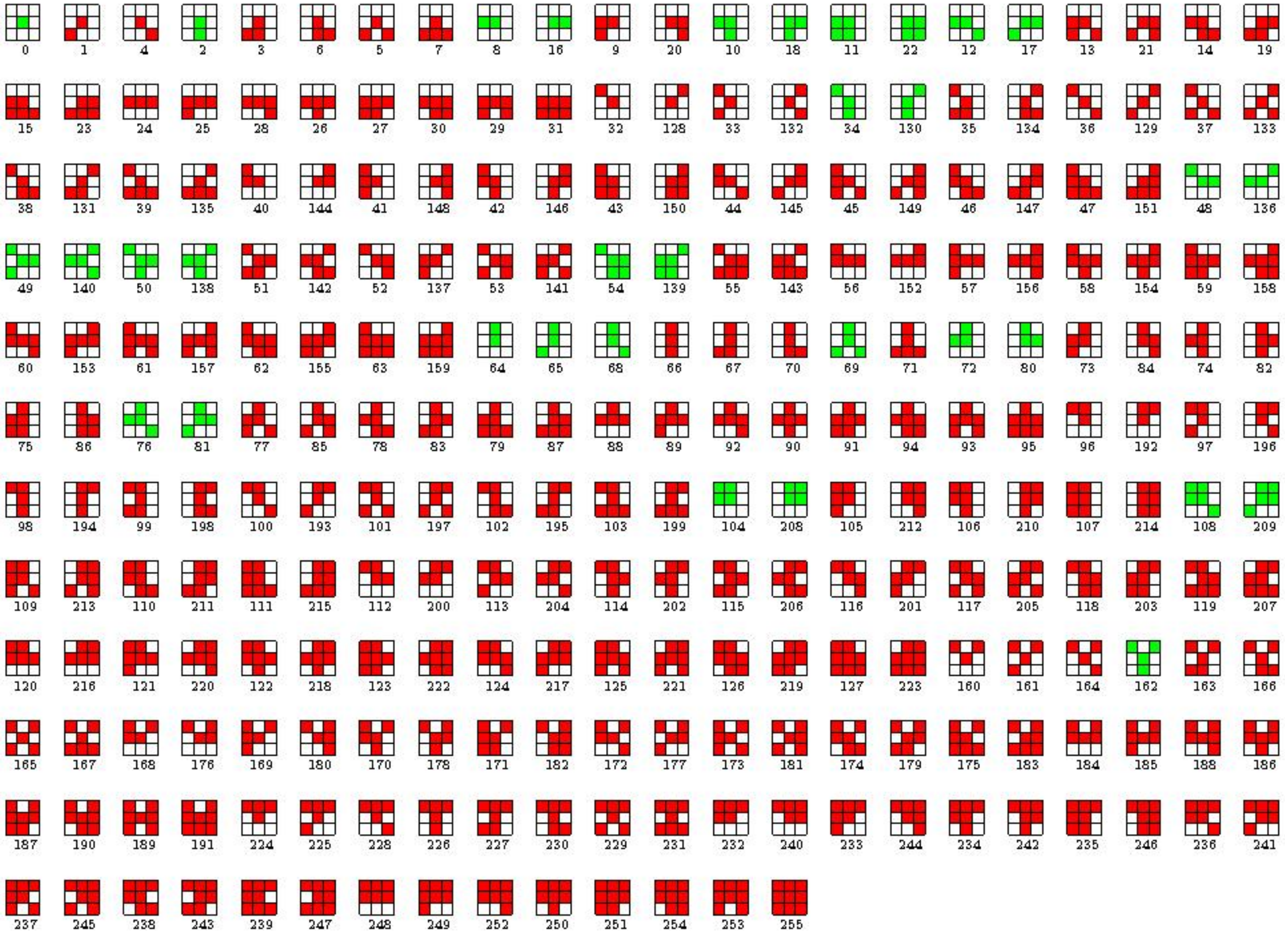

http://cxc.harvard.edu/cal/projects/index.html

Plot of the 256 flight grades that are assigned on-board to each detected event. These 256 events are latter binned into the 7 ASCA grades during ground processing. In order not to saturate telemetry, not all flight grades are telemetered to the ground. The flight grades in green show events that mapped into good ASCA grades (0,2,3,4 and 6) and the flight grades in red show events that are mapped into bad ASCA grades (1,5 and 7).

CENTER FOR ASTROPHYSICS HARVARD & SMITHSONIAN

QE, CTI, Gain

- Quantum Efficiency (QE) is the product of the probability that a photon will transmit through the various layers before reaching the photosensitive depletion region and the probability that the photon will be absorbed by depletion region where it can be detected.
- Charge Transfer Inefficiency (CTI) is caused by degradation of the CCD where charge is trapped in the detector as it is moved to the read out amplifiers. This leads to decreased spectral resolution in the detector, but can be corrected by software.
- Gain is the proportion between an event's pulse height and the detected photon energy. This can vary with detector position and time.
  - nominal ACIS gain is 14.6 eV
  - increasing CTI causes effective gain to drift across the detector
  - gain correction improves accuracy of an event's energy estimation

n.b. CTI is the primary measure of radiation damage on the CCDs

Front- and Back-Illumination

ACIS-S1 and -S3 are back-illuminated CCDs

- more sensitive to soft photons below 2 keV
- noisier with high background

BI CCDs identical to FI CCDs except bulk material thinned and flipped over since soft X-rays absorbed by gate structure.

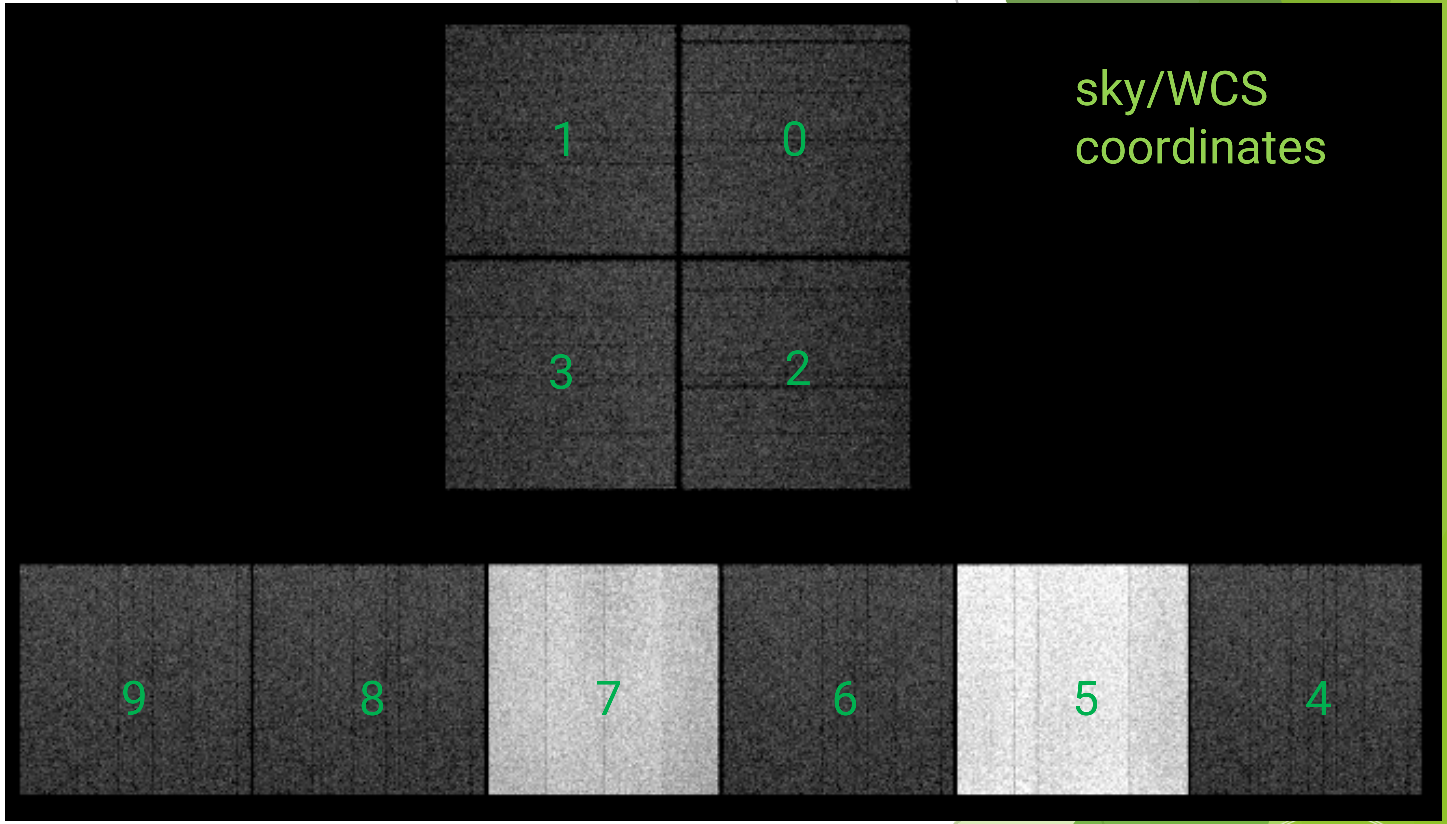

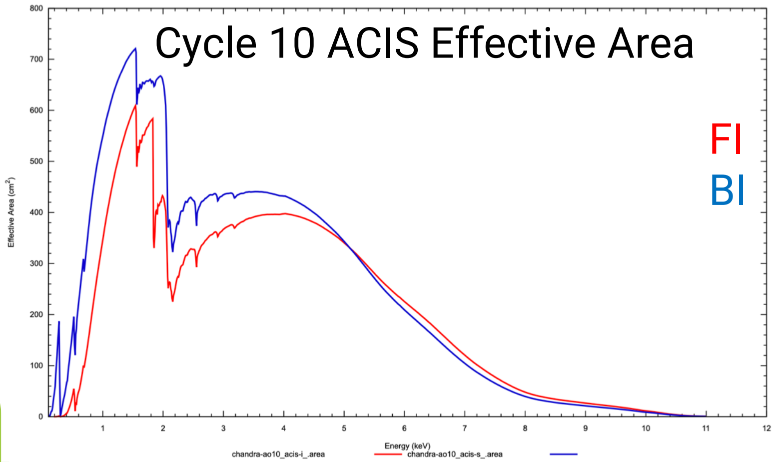

n.b. in practice distinguishing between ACIS-I and ACIS-S is not particularly useful.

OBF and Contamination

- ACIS is also sensitive to optical-band photons
- Optical Blocking Filter (OBF) placed atop ACIS in between the detector and HRMA consisting of polyimide sandwiched between two thin layers of aluminum

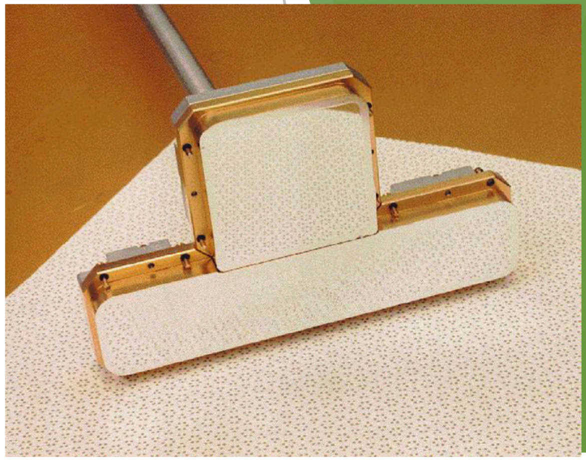

Over time, unidentified contaminant has gradually accumulated on the surface of the OBF that is optically thick to soft X-ray photons, especially below 1 keV and has little effect at higher energies. Below 0.5 keV, quantum efficiency is completely dominated by the contaminant absorption.

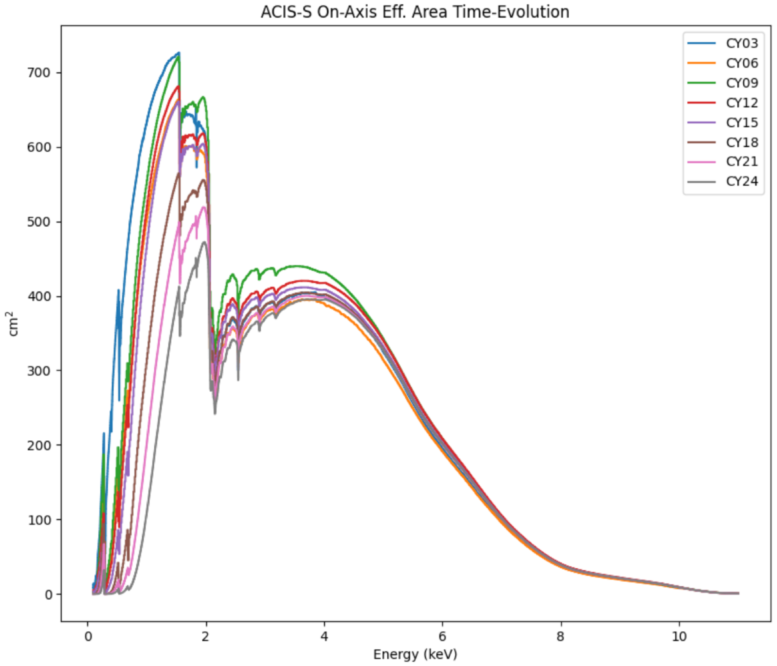

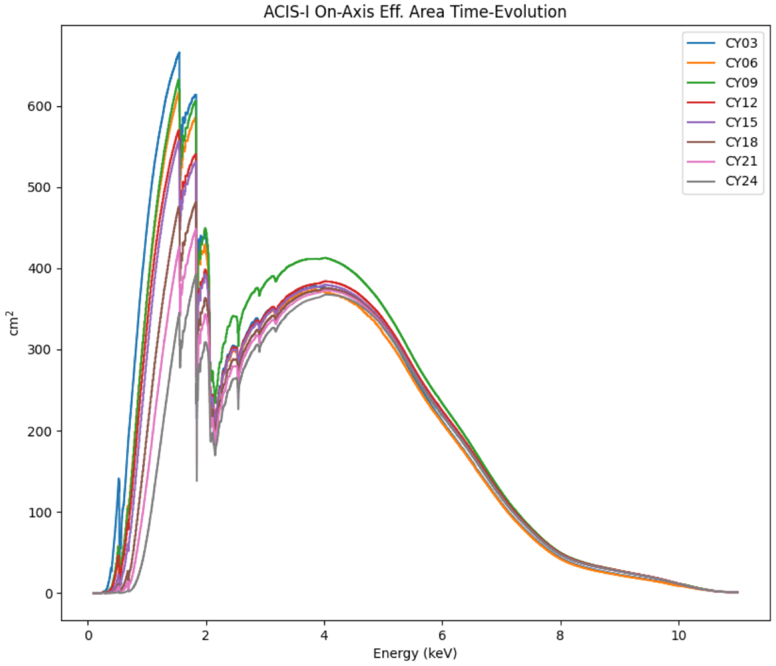

High Resolution Camera

HRC

- microchannel plate detectors
- unlike CCDs with pixel gate structures, surface covered with 10-12.5 µm pores
- angular resolution 0.13175 arcsec/pix
- spectral resolution R~1
- HRC-I FOV 30’x30’
- HRC-S three plates, each 6’x33’

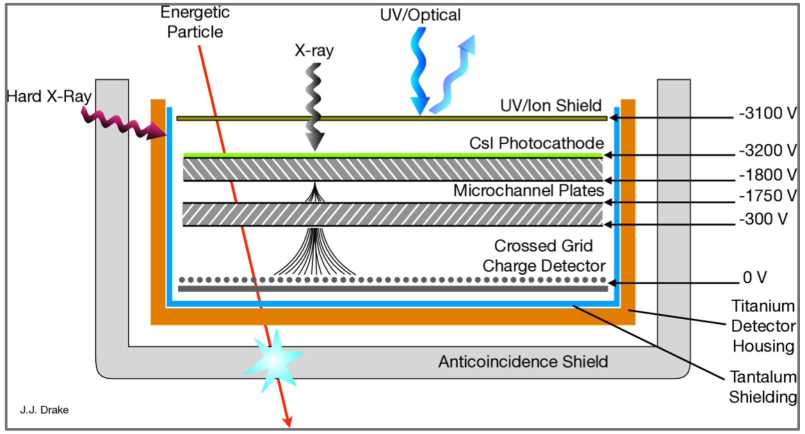

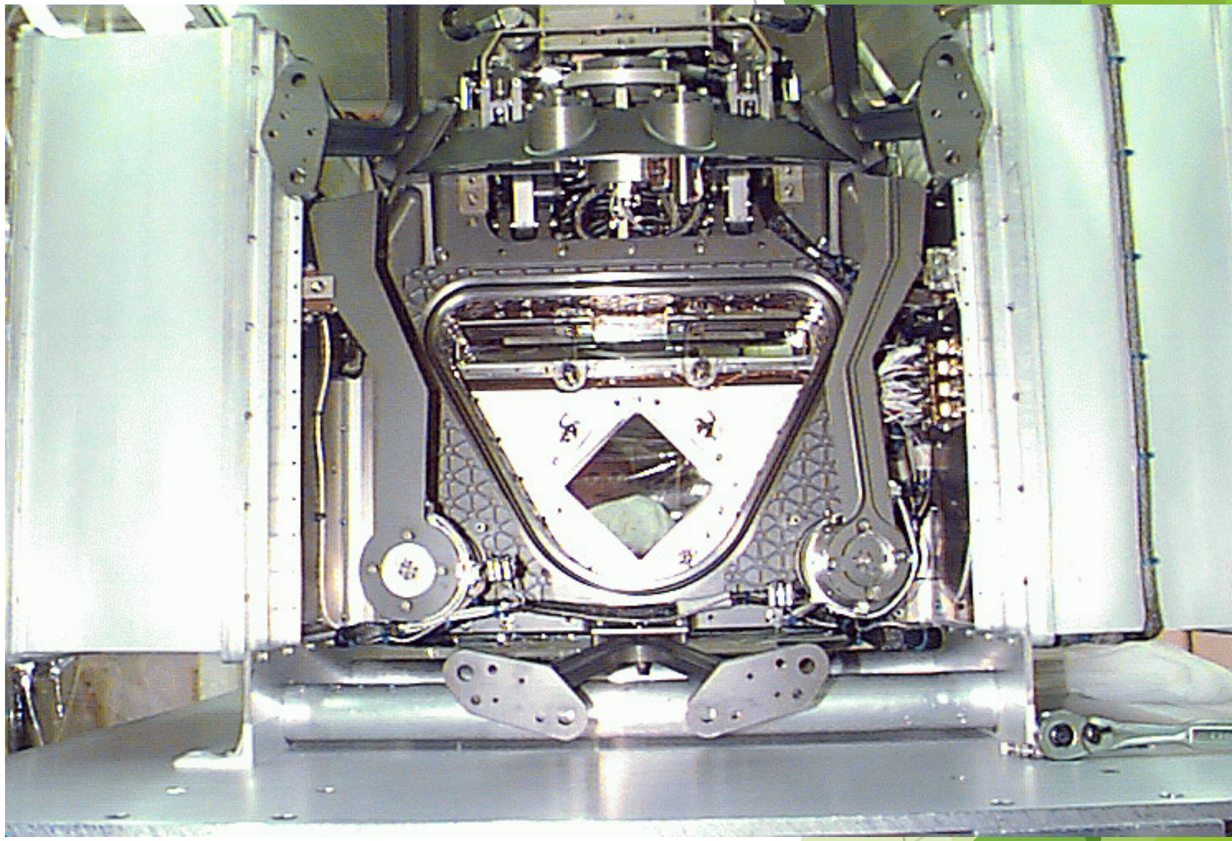

HRC is typically used in very crowded fields where the best position is necessary and/or when timing information is necessary e.g., localize an accreting, millisecond X-ray pulsar

HRC continued…

- the HRC detectors were designed to have a time resolution of 16 μs but a wiring error causes an event's time tag to be the time of the next detected event leading to millisecond-scale timing resolution
  - likely background events (~180 cts/s) primary contribution to diminished timing capabilities
  - time resolution recoverable on-axis in small, central portion on HRC-S for bright sources, $C_{\mathrm{src}} \gg C_{\mathrm{bkg}}$

- generally, handling HRC data is identical to ACIS data. The most notable difference is the lack of energy information in the HRC event file.

Transmission Gratings

The *High-Energy Transmission Grating Spectrometer* and *Low-Energy Transmission Grating Spectrometer* can be separately inserted into the optical path in concert with a detector to perform high-resolution dispersive spectroscopy.

Gratings significantly lowers the effective area!

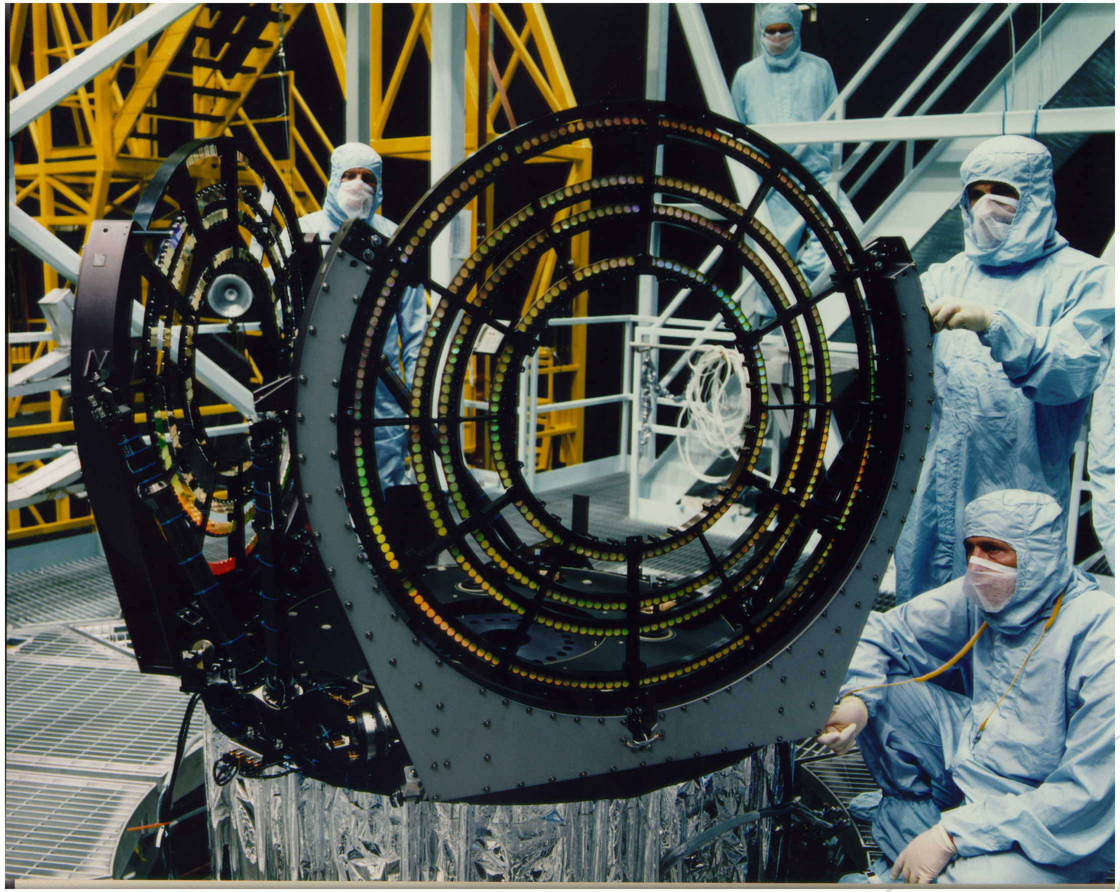

This topic will be covered in-depth on Thursday by Moritz.

High-Energy Transmission Gratings

CHANDRA X-RAY OBSERVATORY

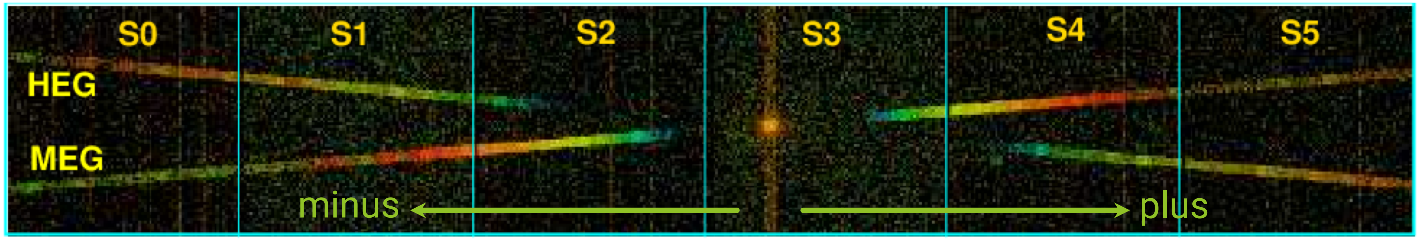

Capella, ObsID 1318 ACIS-S/HETG, detector coordinates, color-coded by energy

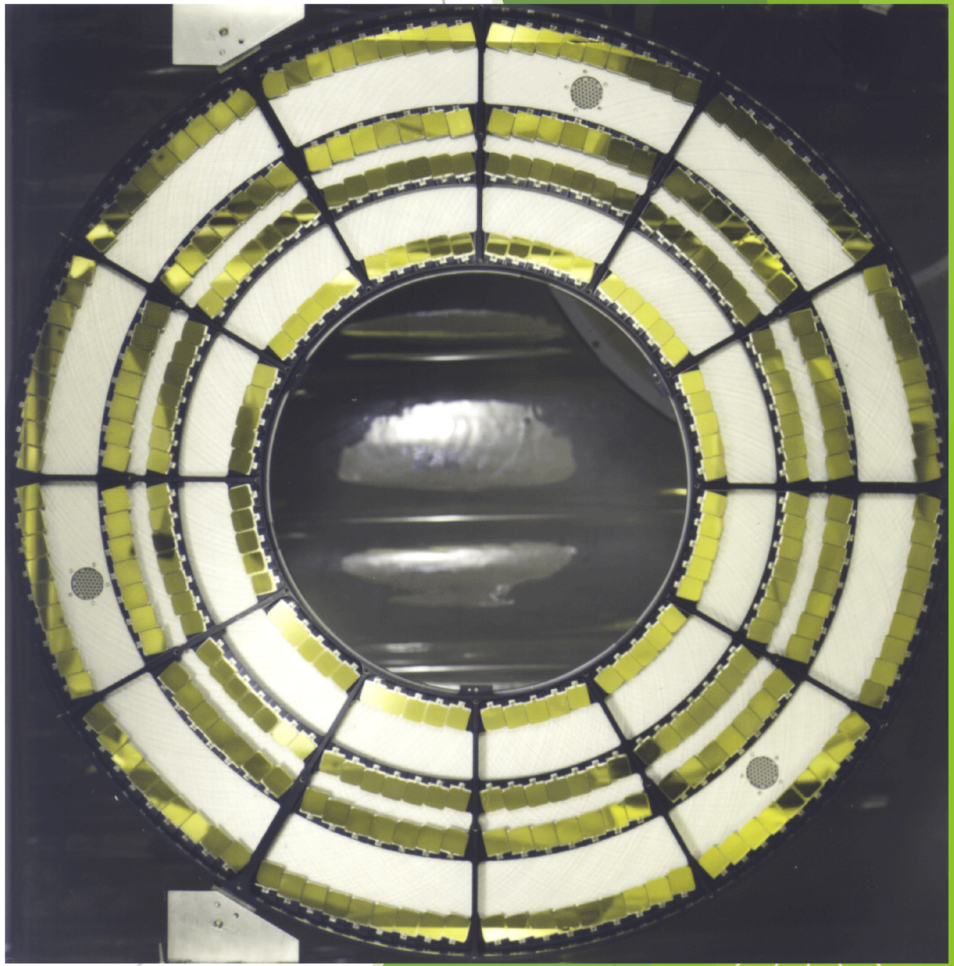

The HETG is composed of:

- High-Energy Grating (HEG, 0.8 – 10.0 keV, 15 – 1.2 Å)
- Medium-Energy Grating (MEG, 0.4 – 5.0 keV, 31 – 2.5 Å)

- the dispersed photons result in an X-shaped pattern on the detector-plane
- zeroth-order can be treated as with regular imaging spectroscopy
- the background level of dispersed events tends to be very low, particularly when used in conjunction with ACIS

CENTER FOR ASTROPHYSICS HARVARD & SMITHSONIAN

Low-Energy Transmission Gratings

The LETG is optimized for high-resolution spectroscopy over the energy bandwidth ~0.09–4 keV (3.1–138 Å) with a resolving power ~1000 at 0.1 keV and ~200 at 1.5 keV.

The large dispersion in energy range of the LETG requires a detector that is physically large in the dispersion direction

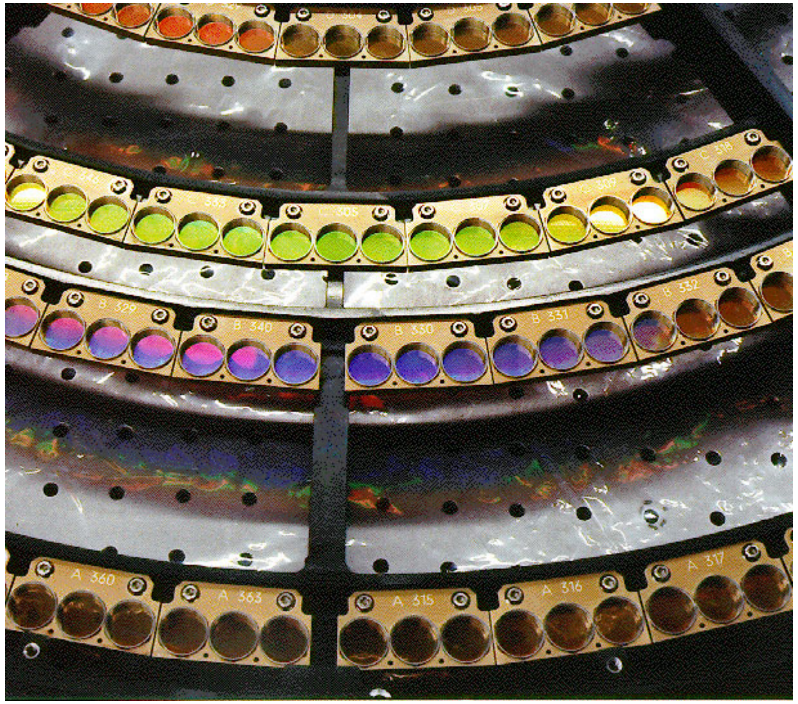

- HRC-S is the only detector aboard that can fully accommodate the LETG-dispersed spectrum
- LETG can also be used with ACIS-S but will have a lower quantum efficiency below ~0.6 keV and the higher dispersed orders will fall beyond the chip edges.

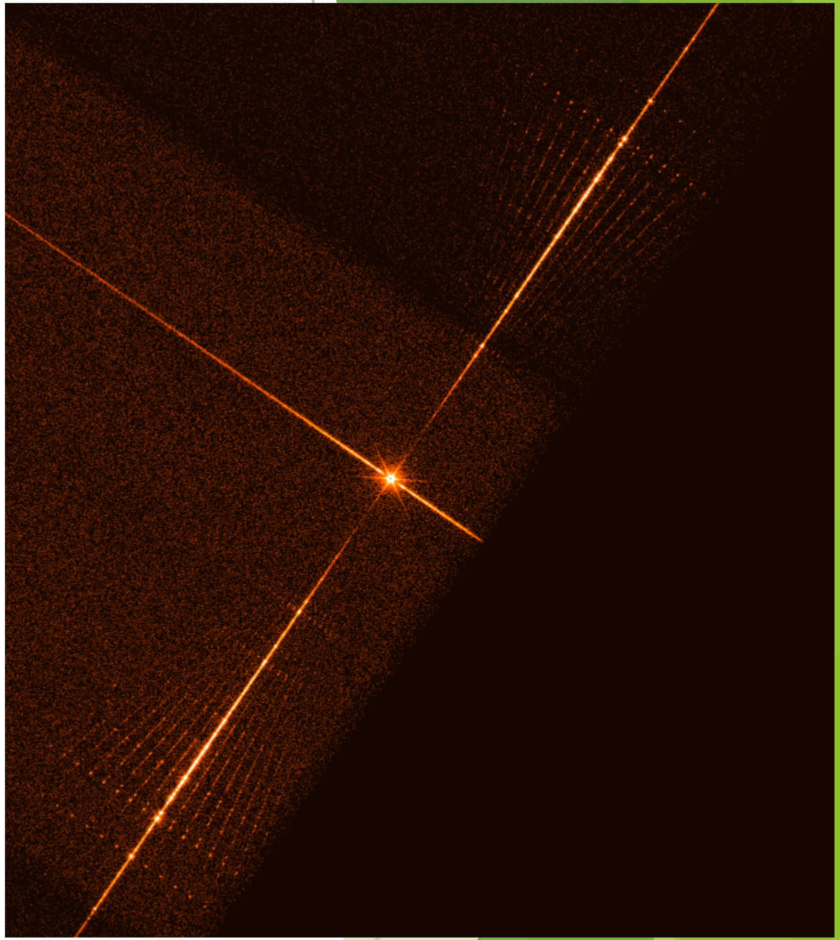

Capella, ObsID 55 ACIS-S/LETG

CHANDRA
X-RAY OBSERVATORY

Whole Bunch of Extra Material

CHANDRA
X-RAY OBSERVATORY

More on ACIS…

	—	HETG	LETG
ACIS-I	8134	1	15
ACIS-S	11926	2008	342
HRC-I	1836	7	64
HRC-S	986	0	666

observed and scheduled as of 2025 May 12

CENTER FOR ASTROPHYSICS
HARVARD & SMITHSONIAN

ACIS Observing Modes

- Timed Exposure
  - events are integrated over a preselected amount of time—a.k.a. the "*Frame Time*"
    - nominal frame time is about 3 seconds, depends on number of active CCDs
    - after frame exposed, charge from the active region of the detector is read out, taking an additional 41 μs
    - frame time shorter than the nominal value results in "deadtime", where no data are taken
      - the nominal amount of time is required for the full frame store read-out process, regardless of the selected frame time
- Alternate Exposure (a.k.a. Interleaved)
  - read-out exposures alternate between a long frame time and a short frame time
- Continuous Clocking
  - uninterrupted data read-out resulting in an effective integrated frame time of 2.85 ms
  - high time resolution comes with the loss of one spatial dimension

CHANDRA X-RAY OBSERVATORY

ACIS Telemetry Data-format Modes

Faint

Event position, arrival time, a signal amplitude, and the signal amplitude in each pixel in the 3×3 event island that determines the event grade

Very Faint (VFaint)

Event position, an arrival time, a signal amplitude, and the signal amplitudes in a 5×5 island. This format is only available with TE-mode and events are graded by the contents of the central 3×3 island.

Graded

Event position, arrival time, a signal amplitude, and the event grade. Event grading and rejection are performed on-board.

CENTER FOR ASTROPHYSICS HARVARD & SMITHSONIAN

CHANDRA X-RAY OBSERVATORY

ACIS Sub-Arrays

Sub-arrays are a subset of the available pixel rows on the active CCDs.

- short nominal frame time, as low as 0.3 s
- reduces observed pile-up
- minimizes deadtime

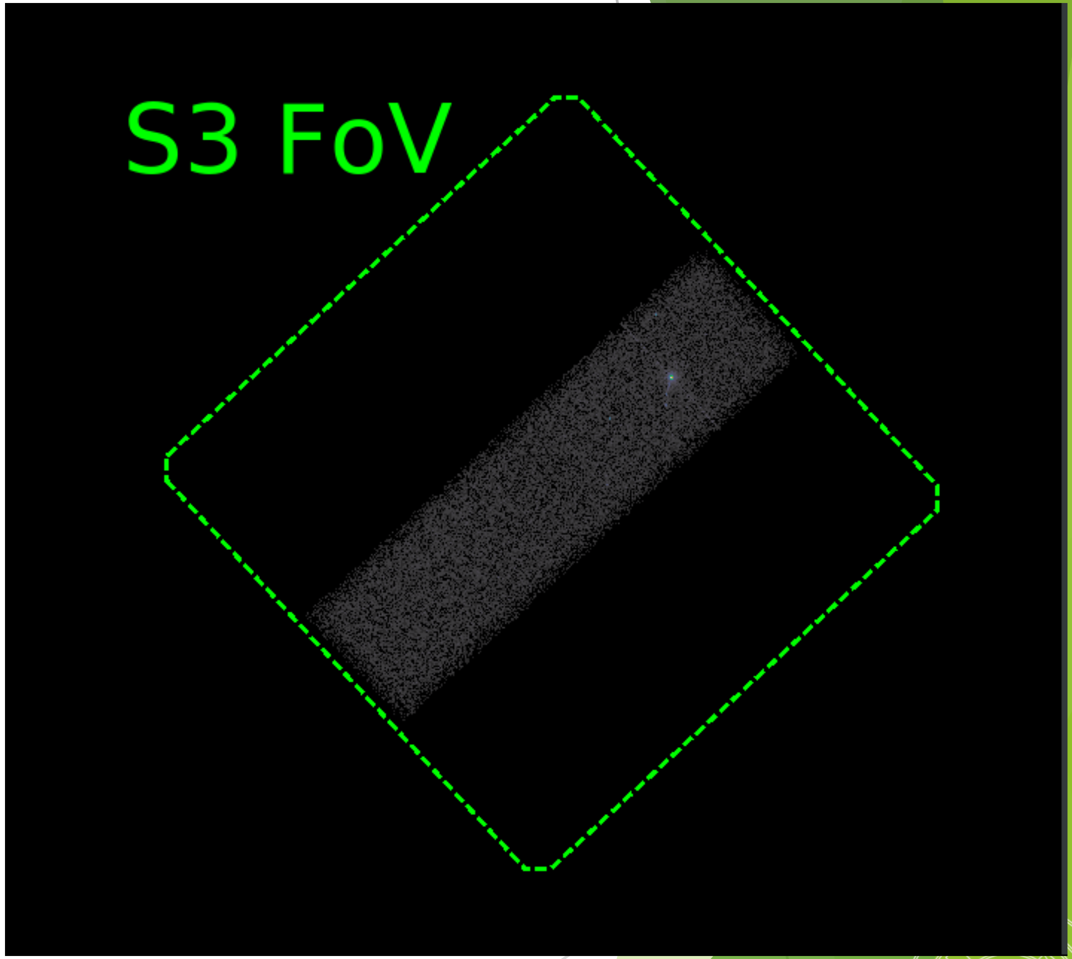

CENTER FOR ASTROPHYSICS
HARVARD & SMITHSONIAN

Readout Streak
a.k.a. Out-of-Time Events

- ACIS does not have a shutter
- during the 40 μs transfer to the frame-store for read-out, events are still detected since the entire chip column is exposed to the sky
- these events detected during read-out have random chip rows as the charge is moved through the electronics, resulting in a cumulative streak

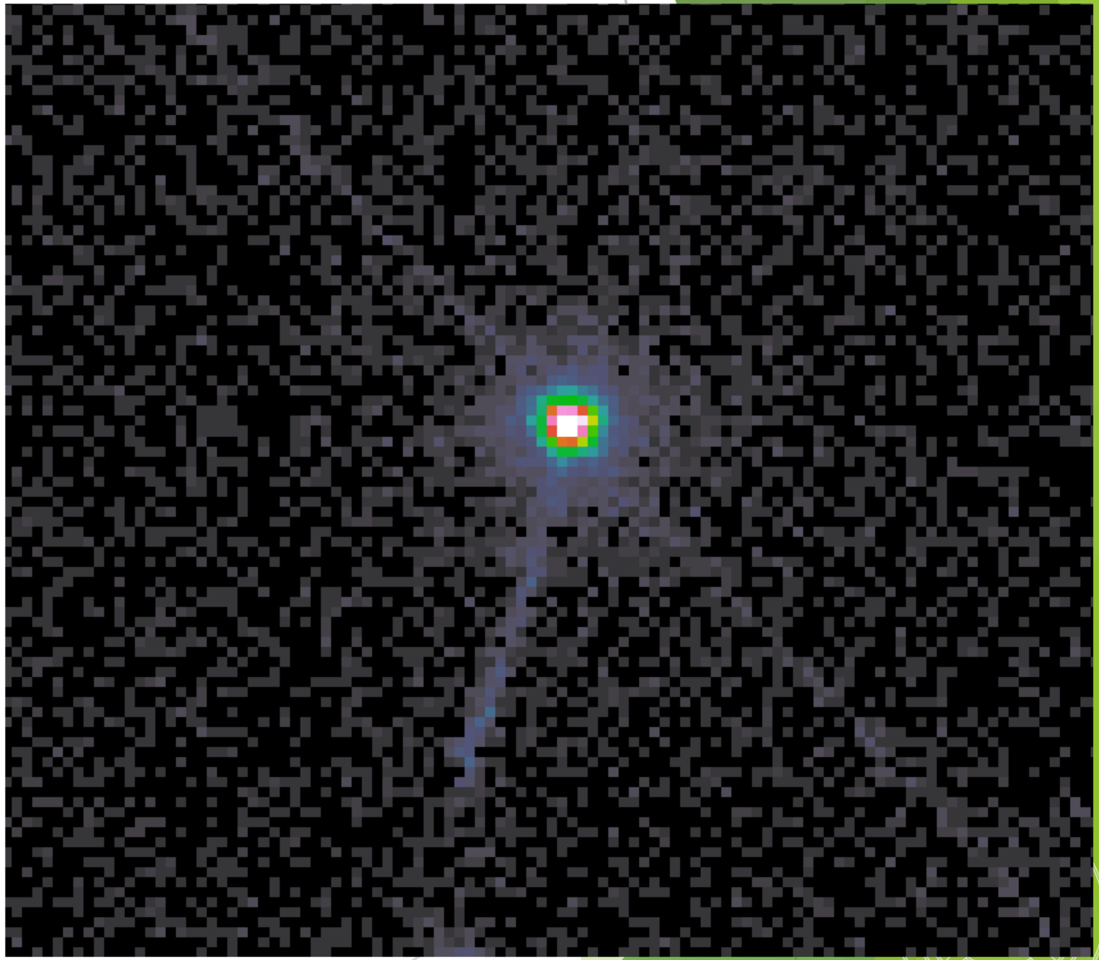

CHANDRA X-RAY OBSERVATORY

Pileup

For a bright source, there is a non-negligible probability for two or more photons to arrive within a few pixels of each other during an integration time. The detector will be unable to distinguish the two events. This phenomena is called "pileup".

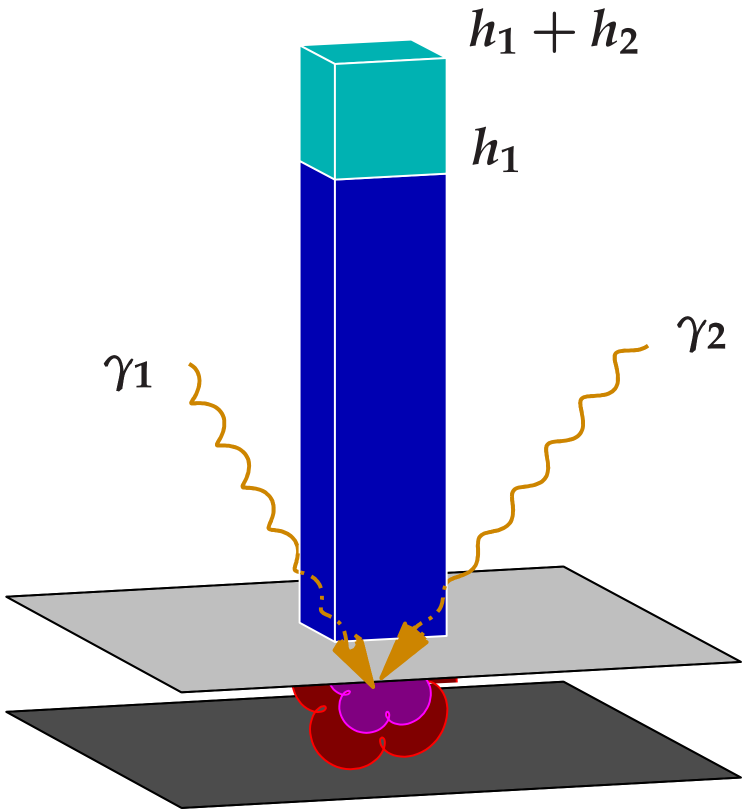

CENTER FOR ASTROPHYSICS HARVARD & SMITHSONIAN

Pileup

Piled up events either identified as a bad event grade of a single event

- inferred event energy approximately the sum of the individual putative event energies
- reduces total number of detected events
- spectral hardening of continuum sources
- distorts PSF

Pileup can be modelled in spectral analysis, but the best strategy is to minimize pileup during an observation.

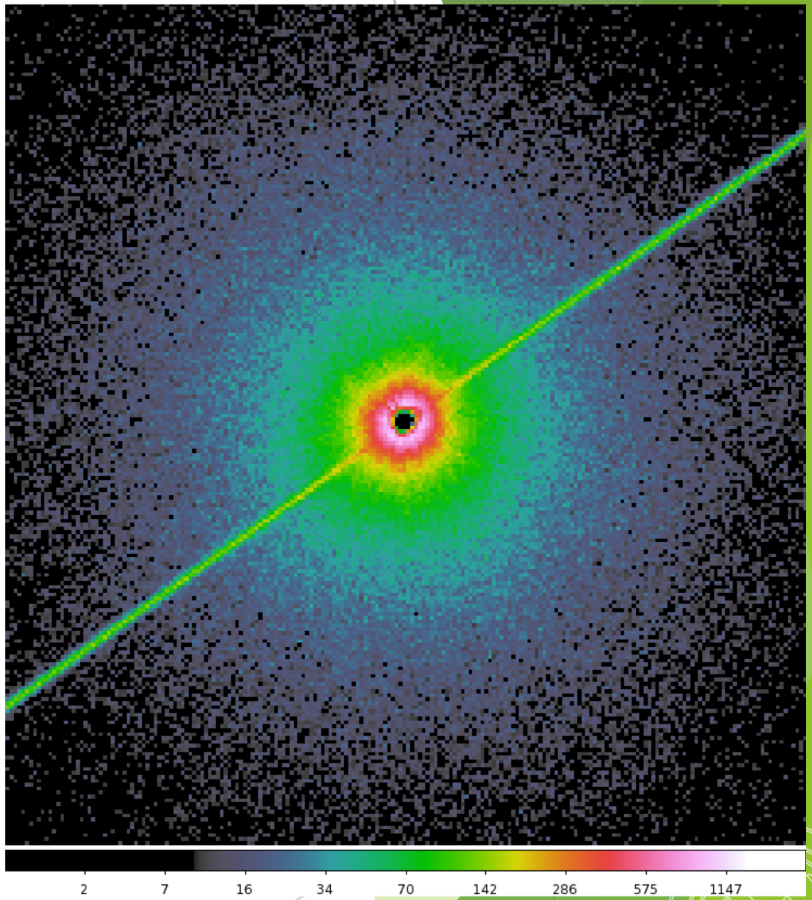

n.b. the presence of a readout streak typically indicates that there is some degree of source pileup

Continuous Clocking Mode

CC-mode

When observing very bright or fast changing sources, both ACIS-S and ACIS-I can be used in CC-mode, which allows for continuous chip read-out at 2.85 ms per row, but loses one spatial dimension.

Because all the events are collapsed onto a single spatial axis the background level is high.

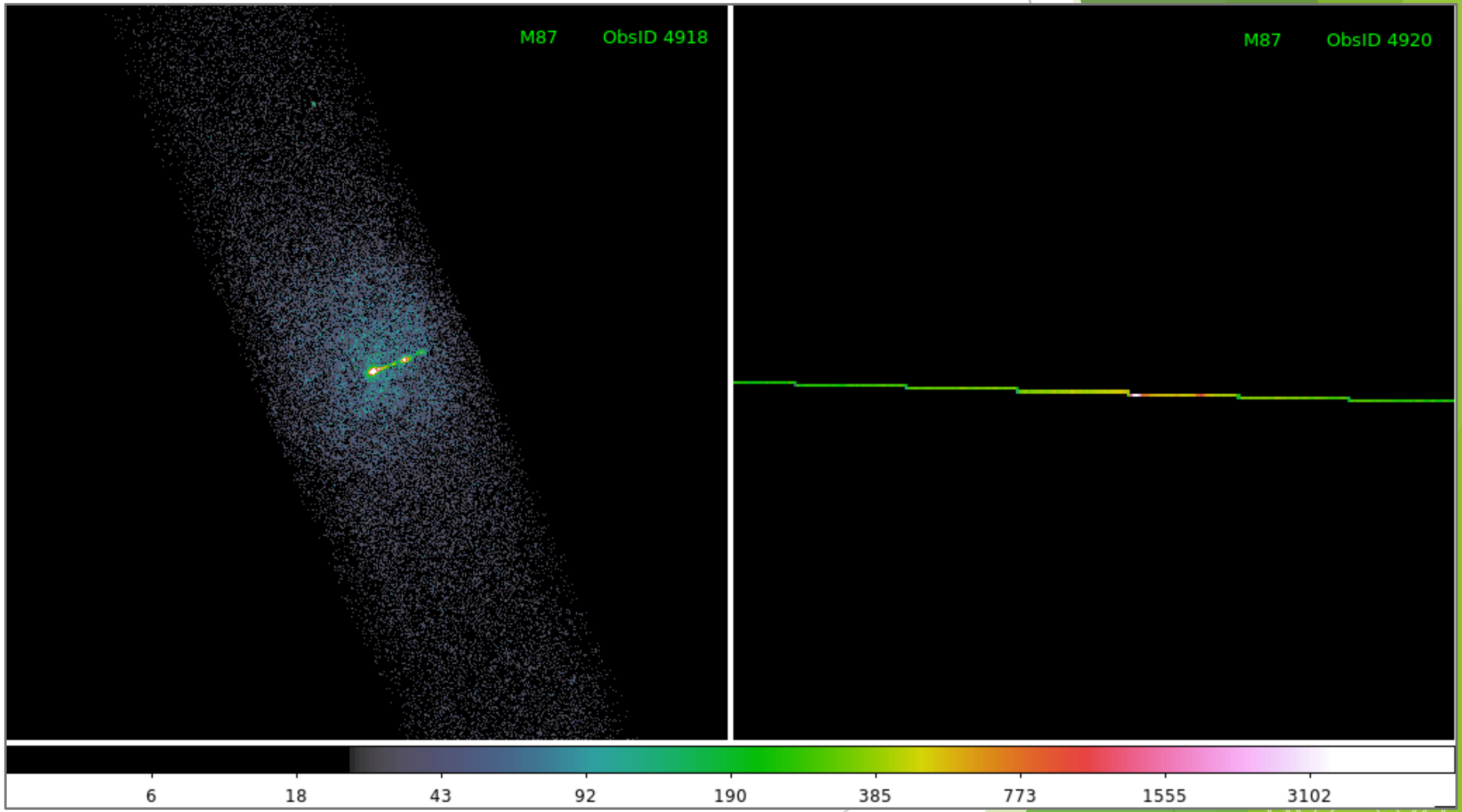

Spatial Windows

- telemetered data mode format determines the data size per event and limiting telemetry rate will saturate and data will be lost until the on-board buffer empties
- bright sources are susceptible to telemetry saturation
  - full frame exposures are dropped resulting in reduce effective observing time
- Dropped ACIS frames can be avoided by onboard event filtering with Graded data mode or applying a spatial window to the read-out data to limit/exclude events in specified portions of the detector from the telemetry stream.
- full frame is still read out by detector

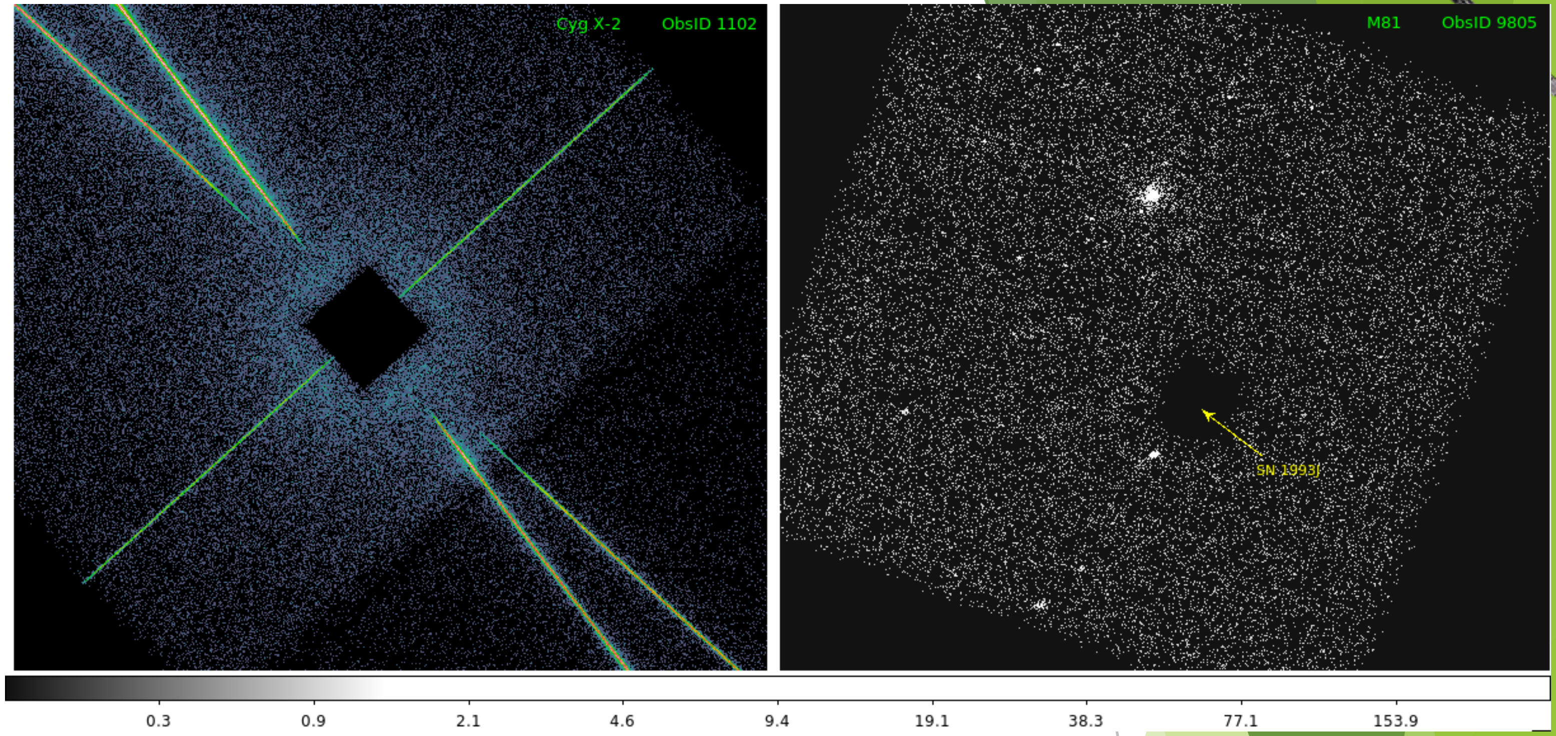

Telemetry Saturation Limits for each ACIS Readout Mode		
Readout Mode	**bits/event**	**events/sec**
CC graded	34	700
CC faint	55	432
TE graded	58	410
TE faint	128	186
TE faint + bias	236	100
TE very faint	320	74

*HRC telemetry limit is 184 events/sec

Energy-Dependent Subpixel Event Repositioning (EDSER)

If the size of the core of the optic's PSF is smaller than the size of the detector pixels near the optical-axis of the telescope, images of sources with small-scale features can be improved by binning on scales smaller than a CCD pixel.

The charge cloud can be smaller than an individual pixel and by using a split event's grade and how its charge cloud interacts with the adjacent pixels, the incident photon position can be localized to better than the pixel center since sky$(x, y) \in \mathbb{R}$.

sub-pixel scales are not calibrated!

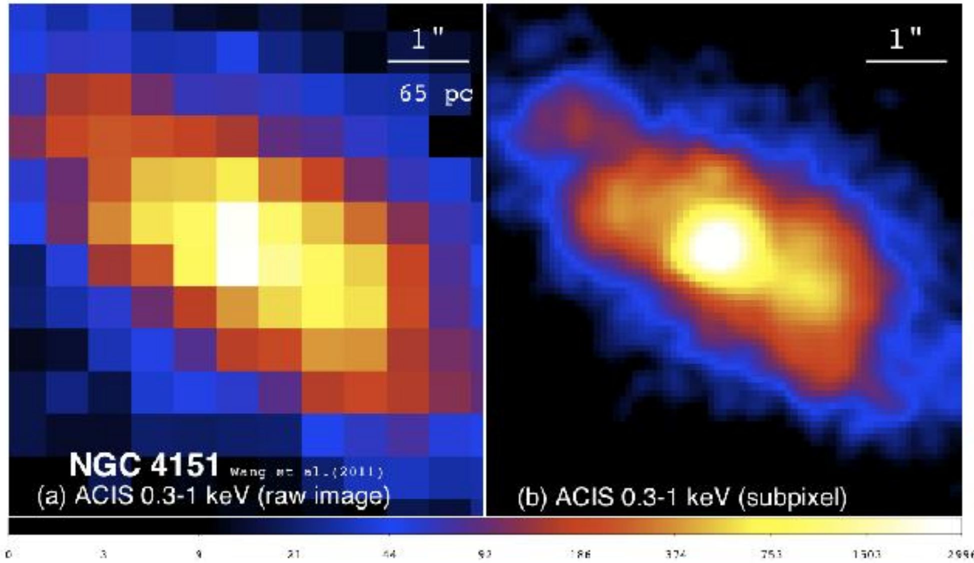

The nucleus of NGC 4151. The left-hand image does not include the effects of a subpixel algorithm and has 0.5 arcsec bins. The right-hand image has a SER applied and has 0.0625 arcsec bins and is smoothed with a FWHM=0.25 arcsec Gaussian for better visualization of faint extended sources (Wang, et al. 2011, ApJ 729, 75)

EDSER algorithm:
Chandra ACIS Subpixel Event Repositioning: Further Refinements and Comparison Between Backside- and Frontside-Illuminated X-ray CCDs; Li et al, ApJ 610 1204

Background Information:
Improvement of the Spatial Resolution of the ACIS Using Split-Pixel Events; Tsunemi et al, ApJ 554 496

Refining Chandra/ACIS Subpixel Event Repositioning using a Backside-Illuminated CCD Model; Li et al, ApJ 590 586

Instrumental & Particle Background

CHANDRA X-RAY OBSERVATORY

- ACIS sensitive to X-ray events >10 keV, but HRMA does not efficiently focus photons $<$ 8 keV; high-energy events assumed to be induced by particles interactions (Hickox & Markevitch, ApJ **645** 95)
- detected X-ray photons can come from fluorescence of the detector's material composition induced by MeV particle collisions
  - "instrumental" and "particle" background are used interchangeably in the literature
- of concern for diffuse, extended source spectroscopy
  - over large area, instrumental effects dominate over celestial background events
  - account for particle background by modelling
  - modelling issue: what are particle spectral responses? They are different than the photon responses, but we don't know what they are.

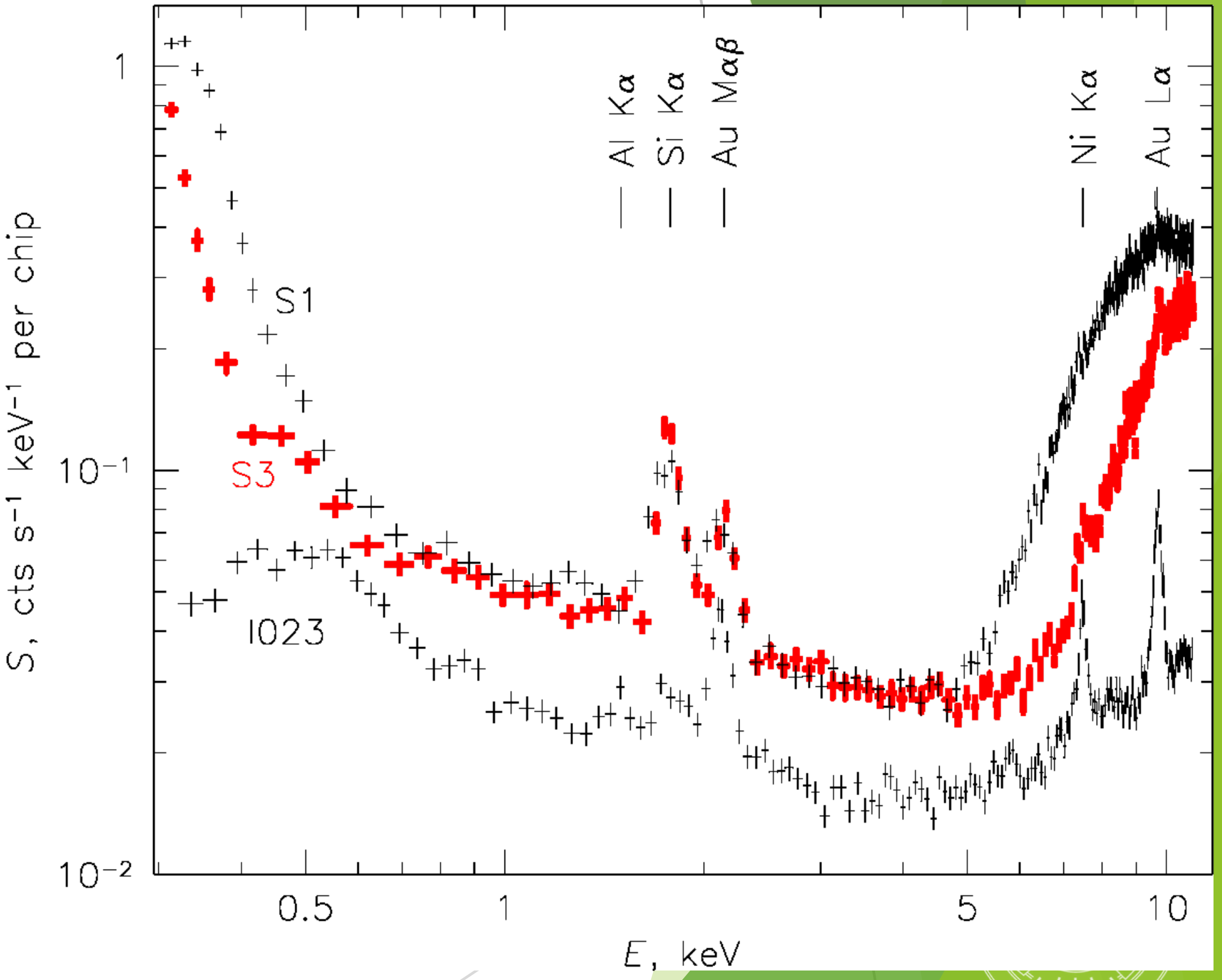

CENTER FOR ASTROPHYSICS HARVARD & SMITHSONIAN

ACIS Raw Frame

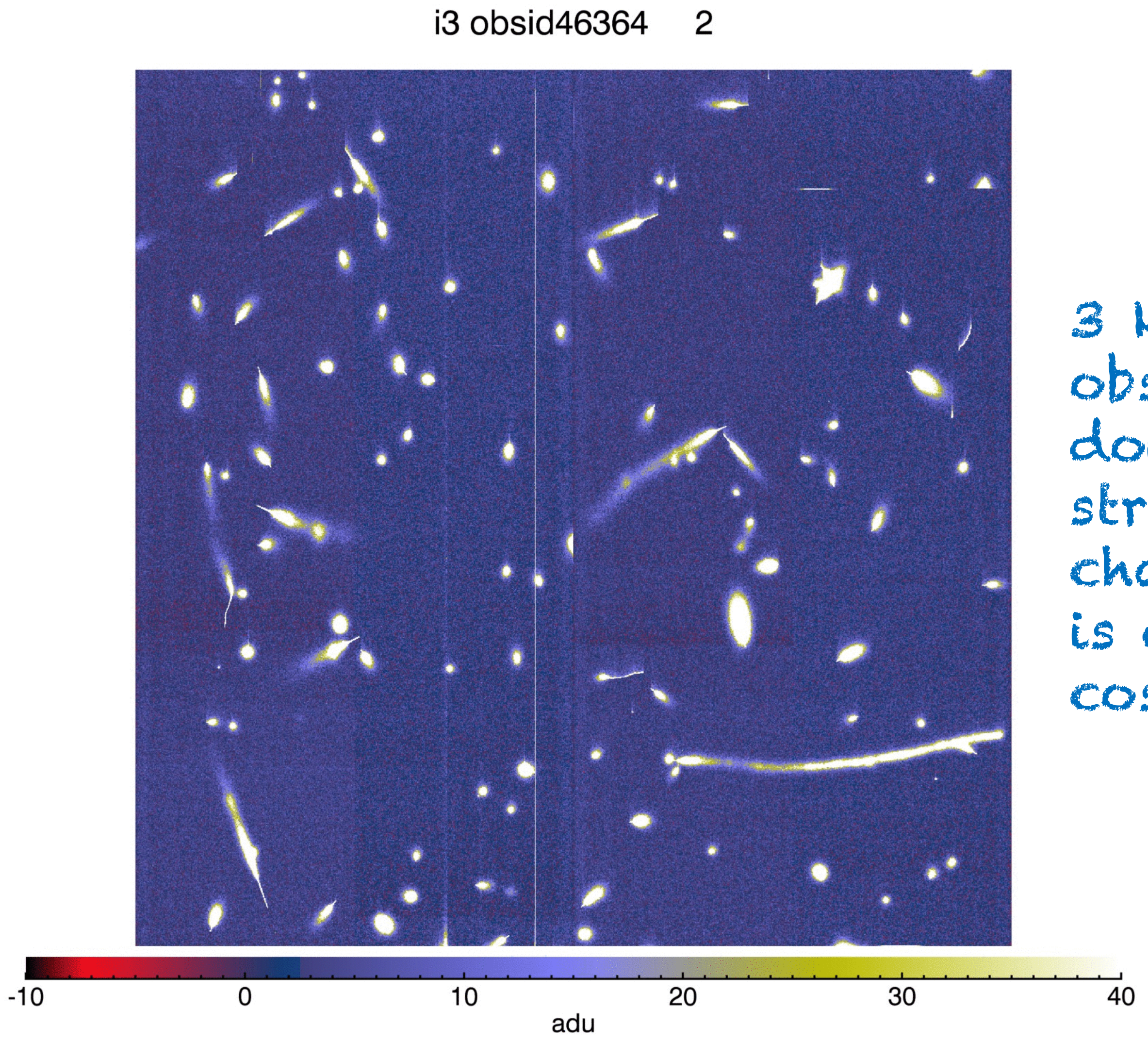

3 ksec engineering observation 46364 – small dots are photon events, streaks and blobs are charged particles; the signal is dominated by high-energy cosmic rays

Taking Advantage of Chip Gaps: V404 Cyg

Light Echoes: ObsID 17704 (ApJ 825 15)

X-ray Binary Spectra: ObsID 17696, 17697 (ApJ 813 L37)

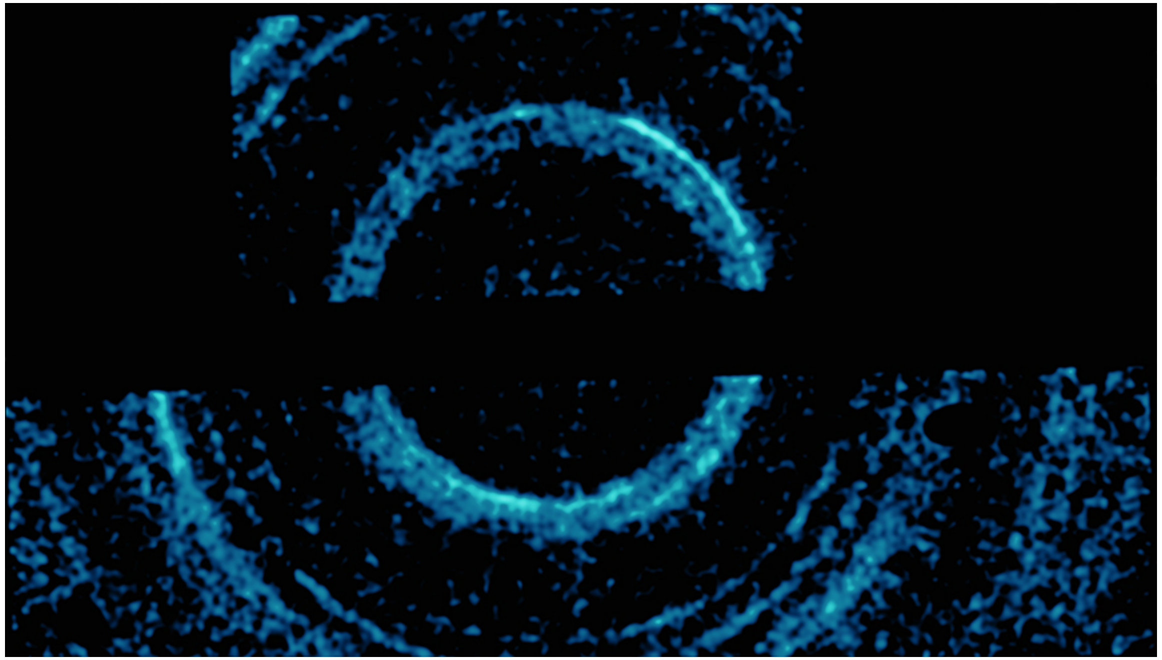

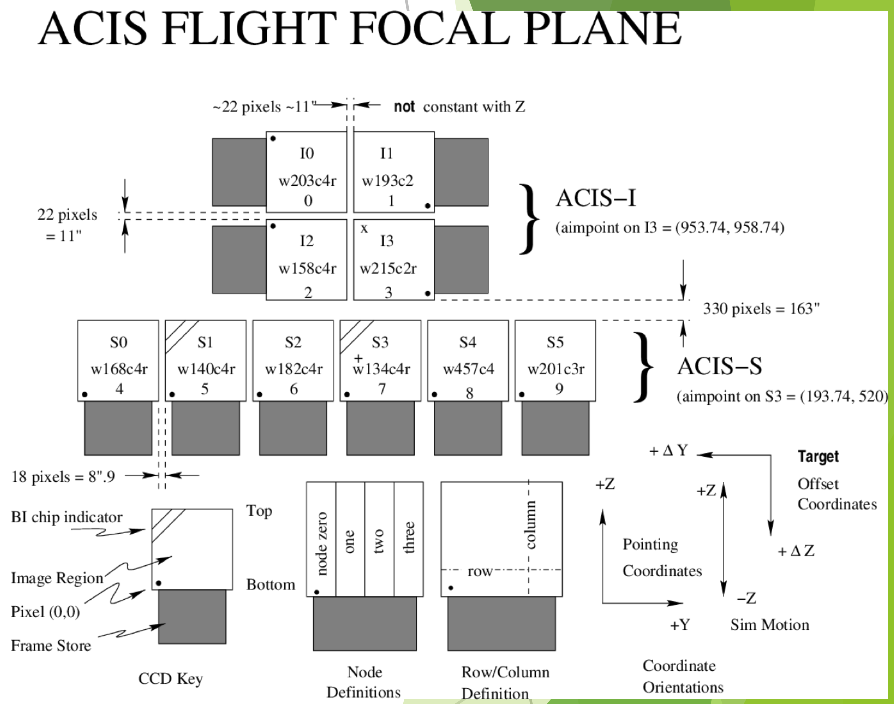

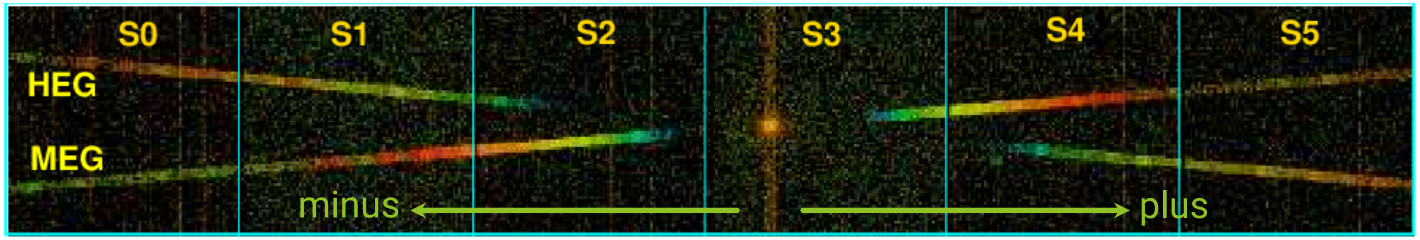

place zeroth-order in gap with HETG/CC-mode to distinguish MEG and HEG dispersed events

CHANDRA X-RAY OBSERVATORY

Backup Slide—Wolter Configurations

- All three configurations are equivalent in optical performance, the main difference is the ratio of the focal length to total system length.
  - Type I has a system length greater than the focal length
  - Type II has a large focal length, which can exceed the system length; grazing incidence equivalent to a Cassegrain
  - Type III has the shortest focal length
- The design most commonly used by X-ray astronomers is the Type I since it has the simplest mechanical configuration and can be nested to increase the effective area with high on-axis angular resolution
- Type II provides longer focal length for but off-axis suffers much more blurring, so used as a narrow-field imager or for dispersive spectrometry
- Type III never used for X-ray astronomy (yet).

Aschenbach, B. *Reports on Progress in Physics*, 48 579-629

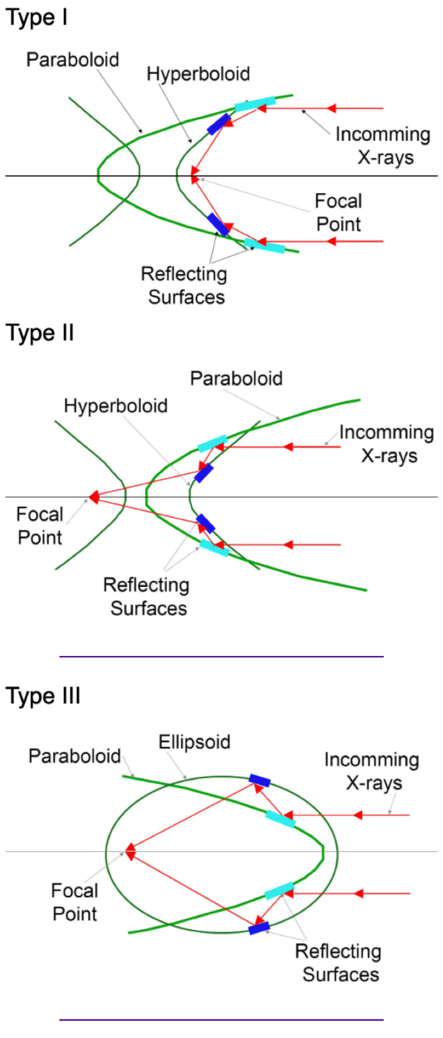

The Wolter X-ray telescope designs.
(Credit: NASA's Imagine the Universe)

CENTER FOR ASTROPHYSICS HARVARD & SMITHSONIAN

X-ray Mirror Technologies

an aside…

Virtually all focusing X-ray telescopes built and proposed use a Wolter I or modified Wolter I configuration since it has the simplest mechanical configuration.

- HRMA uses classical mirrors which can be figured very precisely
  - limited by thickness and mass of mirror shells ⇒ low collecting area
  - resource intensive and monetarily very expensive
- Thin Foil mirrors can approximate the Wolter I geometry
  - light-weight, thin metals, ~170 μm thick; mass produced and stacked
  - poor angular resolution on the order of a few arcminutes
- Replication by electroforming metal shell
  - high cost and relatively high mass to geometric area, ~0.5 mm thick
  - good angular resolution of several-tens of arcseconds and readily stackable; economy of scale w.r.t. classical optics